HHS Public Access

Author manuscript

Acc Chem Res. Author manuscript; available in PMC 2022 April 21.

Published in final edited form as:

Acc Chem Res. 2021 September 07; 54(17): 3476–3490. doi:10.1021/acs.accounts.1c00368.

Ti-Catalyzed and -Mediated Oxidative Amination Reactions

Ian A. Tonks*

Department of Chemistry, University of Minnesota – Twin Cities, 207 Pleasant St SE, Minneapolis, MN 55455

CONSPECTUS:

Titanium is an attractive metal for catalytic reaction development: it is earth abundant, inexpensive, and generally nontoxic. However—like most early transition metals—catalytic redox reactions with Ti are difficult, owing to the stability of the high-valent Ti^{IV} state. Understanding the fundamental mechanisms behind Ti redox processes is key for making progress toward potential catalytic applications. This *Account* will detail recent progress in Ti-catalyzed (and mediated) oxidative amination reactions that proceed through formally Ti^{II}/Ti^{IV} catalytic cycles.

This class of reactions is built off of our initial discovery into Ti-catalyzed [2+2+1] pyrrole synthesis from alkynes and azobenzene, where detailed mechanistic studies have revealed important factors that allow for catalytic turnover despite the inherent difficulty of Ti redox. Two important conclusions from mechanistic studies are that (1) low valent Ti intermediates in catalysis can be stabilized through coordination of π-acceptor substrates or products, where they can act as “redox-noninnocent” ligands through metal-to-ligand π-backdonation; and (2) reductive elimination processes with Ti proceed through π-type electrocyclic (or pericyclic) reaction mechanisms rather than direct σ-bond coupling.

The key reactive species in Ti-catalyzed oxidative amination reactions is a Ti imido (Ti≡NR), which can be generated from either aryl diazenes (RN=NR), or organic azides (RN_3). These Ti imidos can then undergo [2+2] cycloadditions with alkynes, resulting in intermediates that can be coupled to an array of other unsaturated functional groups including alkynes, alkenes, nitriles, and nitrosos. This basic reactivity pattern has been extended into a broad range of catalytic and stoichiometric oxidative multicomponent coupling reactions of alkynes and other reactive small molecules, leading to multicomponent syntheses of various heterocycles and aminated building blocks.

For example, catalytic oxidative coupling of Ti imidos with two different alkynes leads to pyrroles, while stoichiometric oxidative coupling with alkynes and nitriles leads to pyrazoles. These heterocycle syntheses often yield substitution patterns that are complementary to classical condensation routes, and provide access to new electron-rich, highly substituted heteroaromatic scaffolds. Further, catalytic oxidative alkyne carboamination reactions can be accomplished via reaction of Ti imidos with alkynes and alkenes, yielding α,β-unsaturated imine or cyclopropylimine building blocks. New catalytic and toichiometric oxidative amination methods such as alkyne α-diimination, isocyanide imination, and ring-opening oxidative amination of

***Corresponding Author** itonks@umn.edu.

strained alkenes are continuously emerging as a result of better mechanistic understanding of Ti redox catalysis.

Ultimately, these Ti-catalyzed and -mediated oxidative amination methods demonstrate the importance of examining often-overlooked elements like the early transition metals through the lens of modern catalysis: rather than a lack of utility, these elements frequently have undiscovered potential for new transformations with orthogonal or complementary selectivity to their late transition metal counterparts.

Graphical Abstract

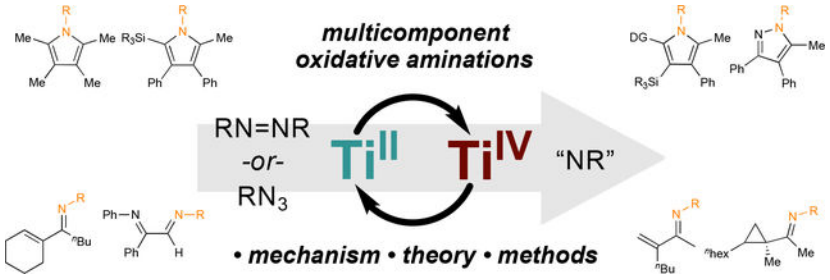

Authors are required to submit a graphic entry for the Table of Contents (TOC) that, in conjunction with the manuscript title, should give the reader a representative idea of one of the following: A key structure, reaction, equation, concept, or theorem, etc., that is discussed in the manuscript. Consult the journal's Instructions for Authors for TOC graphic specifications.

INTRODUCTION

Nitrogen-based functional groups are ubiquitous in bioactive molecules.[5,6] Recently, powerful methods have evolved around new ways of constructing C-N bonds, including alkene hydroamination,[7,8] aziridination,[9] oxidative C-H amination,[10] and multicomponent cycloadditions.[11] To a large extent, this impressive development has been the domain of late transition metals (LTMs), raising the question of the role that early transition metals (ETMs) such as Ti can have in engendering new amination reactions.

ETMs have the potential to access different structures (*e.g.* metal-ligand multiple bonds) and elementary reaction steps than LTMs, potentially enabling new, orthogonal bond-forming strategies.[12] ETMs are also earth abundant: the crustal concentration of Ti is greater than all other transition metals combined, Fe excluded.[13] There is significant opportunity to reinvestigate this often-overlooked part of the transition series through the lens of modern catalysis.[14] In fact, catalysis with Ti^{III}-based reagents has experienced a renaissance owing to increased interest in/understanding of selective radical-based strategies.[15–18]

While there are myriad examples of Ti-catalyzed[15] or stoichiometric[19] reduction reactions, Ti-catalyzed *oxidation* reactions involving metal-centered 2-electron redox are rare, owing to the difficulty in reduction of Ti^{IV} to Ti^{II}.[20] Nonetheless, developments in redox noninnocent ligands[21] over the past 20 years have made ETM redox catalysis an attractive target.

This *Account* will explore recent developments in Ti-catalyzed and -mediated oxidative amination reactions, using mechanistic insight to explain fundamental principles of catalysis and motivate selective reaction development. These oxidative aminations are built off of the (1) reactivity of Ti≡NR imido complexes, which undergo [2+2] cycloaddition[16] with alkynes; and (2) facile bimolecular cleavage of N=N bonds in aryl diazenes by Ti^{II}. Based on this chemistry, diverse multicomponent reactions have been developed that yield important heterocycles and aminated building blocks (Figure 1).

CATALYTIC [2+2+1] SYNTHESIS OF PYRROLES

In 2016, we reported the formal [2+2+1] synthesis of pyrroles (**1**) from alkynes and azobenzene, catalyzed by $py_3TiCl_2(NPh)$ (Figure 2A).[1] This reaction was significant as the first example of catalytic oxidative C-N bond formation with Ti. Tethered diynes (**1a**, **1b**) and simple alkynes (**1c**) undergo reactions with equal efficiency (Figure 2B). Unsymmetric internal alkynes (**1e, 1f**) yield regioisomeric mixtures, where the product distribution is often statistical. Terminal alkynes (**1g, 1h**) also yield regioisomeric mixtures but have a strong preference for formation of 2,4-disubstituted product **1**. Qualitatively, the effect of alkyne structure on reaction rate is terminal (**1g**, **1h**) > polarized (**1f**) > internal dialkyl (**1c**) > internal diaryl (**1d**). In the case of highly reactive terminal and polarized alkynes, an excess of aryl diazene is sometimes needed to suppress unwanted alkyne cyclotrimerization.

This catalytic [2+2+1] pyrrole synthesis has formed the underpinnings for a large array of oxidative nitrene transfer reactions that have been developed in our labs, and mechanistic studies have been a key driver in their development. As a foundation for later work, details of each step of the mechanism will be discussed first along with historical context and computational studies, before returning to new reaction discovery.

[2+2+1] pyrrole synthesis is an extension of ETM imido-catalyzed alkyne hydroamination.[8] In Ti-catalyzed alkyne hydroamination, [2+2] Ti≡NR (**IM1**) + alkyne cycloaddition (**TS1**) leads to an azatitanacyclobutene (**IM2**), which undergoes protonolysis by a primary amine to liberate enamine (imine) **3** (Figure 3B). Inspiration for [2+2+1] pyrrole synthesis was borne out of a study of $(ONO)TiBn_2$ (**2**) catalyzed 2-butyne hydroamination (Figure 3A).[23] Reactions with excess 2-butyne catalyzed by **2** resulted in trace amounts of pyrrole **1i** and C_6Me_6 **4**. We speculated that these sideproducts were generated through 2nd alkyne insertion into **IM2**, leading to an azatitanacyclohexadiene (**IM3**) that underwent reductive elimination to form **1i** and a Ti^{II} species which cyclotrimerized remaining 2-butyne to **4**. This hypothesis led to the discovery of simple Ti complexes (*e.g.* $py_3TiCl_2(NPh)$) and oxidants (aryl diazenes,[1] later organic azides[24]) capable of closing the catalytic cycle for pyrrole production.

[2+2+1] Mechanism – Overview.

A summary of the mechanism of Ti-catalyzed formal [2+2+1] pyrrole synthesis[2] is presented in Figure 4, along with rate laws derived from variable time normalization analysis[25] (VTNA). Computational studies[2,26] indicate that the active species has 1 coordinated pyridine (**IM4**), although there may be complex/changing speciation resulting from reversible pyridine coordination to various intermediates along the cycle.

First, Ti^{IV} imido **IM4** undergoes [2+2] cycloaddition with an alkyne to form azatitanacyclobutene **IM5**. Next, a second alkyne inserts into **IM5** to form azatitanacyclohexadiene **IM6** in the rate-determining step. Reductive elimination from **IM6** next yields a Ti^{II} intermediate, either free or as "masked" Ti^{II} backdonating to the bound pyrrole (**IM7**). **IM7** can then either unproductively trimerize alkyne or be trapped by azobenzene to form Ti^{II} η^2-azobenzene adduct **IM8**, which disproportionates into a Ti^{IV} imido (**IM4** and **IM4-Dimer**) to close the cycle. Reoxidation of **IM7** is facile, and examples of Ti imido synthesis by Ti^{II} azobenzene disproportionation/oxidation go back several decades.[27,28] Disproportionation is likely bimetallic although the exact mechanism (homodimerization of **IM8** as drawn, or reaction[29] of **IM8** with free Ti^{II}) remains unclear. Disproportionation is irreversible (no diazene crossover has been observed), likely owing to the formation of strong Ti≡NR bonds. Half order dependence on [Ti] indicates an equilibrium between the precatalyst, **IM4**, and **IM4-Dimer**, consistent with kinetic analyses of Ti-catalyzed alkyne hydroamination[30,31] where Ti imidos are well-known to dimerize.[8]

Second Alkyne Insertion.

Despite many studies of [2+2] cycloaddition of Ti imidos, there are only two examples of alkyne insertion into group 4 azametallacyclobutenes like **IM5** (Figure 5). First, Walsh and Bergman[32] reported that reaction of Zr *bis*(amide) **5** with excess MeCCMe resulted in [2+2] cycloaddition and 2nd alkyne insertion to **6**. Mountford[33] isolated **8** from reaction of **7** with excess arylacetylene. Similarly, Odom reported that Mo and W *bis*(imido)s undergo double reaction with cyclooctyne to form azametallacycloehexadienes which liberate pyrrole upon heating.[34]

Insertions of other unsaturated species (*e.g.* nitriles,[35] aldehydes,[36] and imines.[37]) into azatitanacyclobutenes have also been reported. Notably, Odom has reported a versatile class of catalytic iminoamination reactions *via* isocyanide insertion.[38,39] Cloke reported a stoichiometric [2+2+1] synthesis of 1,2,4-azadiphosphole via double phosphaalkyne reaction with $py_3TiCl_2(N^tBu)$.[40]

In [2+2+1] pyrrole synthesis, a second alkyne inserts into **IM5** since (unlike in hydroamination) there is no amine for protonolysis. The 2nd alkyne insertion is more kinetically challenging than [2+2] cycloaddition (or protonolysis), owing to sterically-encumbered 6-coordinate **TS3**. For reactions of dialkylacetylenes catalyzed by py_3TiCl_2(NPh), kinetic (2nd order [EtCCEt]) and computational analysis (Figure 4, **TS3** $\Delta G^{\ddagger}$ = 29.6 kcal/mol *vs.* **TS2** $\Delta G^{\ddagger}$ = 22.0 kcal/mol; MeCCMe) indicate 2nd insertion is rate-determining.

C-N Reductive Elimination.

Ti organometallics are more likely to undergo H-abstraction[41] or radical reaction[42] than σ-bond reductive elimination. Thus, it is surprising that **IM6** undergoes *facile* C-N reductive elimination (Figure 4, **TS4**).

Since reductive elimination occurs after rate-limiting **TS3**, this step has only been examined computationally. Comparative free energy profiles for reductive elimination from two

major computational studies[2,26] are presented in Figure 6. Although significant free energy differences arise between these models (resulting from different levels of theory and computational approaches: gas-phase geometry optimizations followed by single-point calculations[26] *vs.* initial geometry optimization in solvent[2]) it is clear that C-N reductive elimination is a low barrier process (**TS4** $\Delta G^{\ddagger}$ = 20.1 or 10.6 kcal/mol). There is debate on whether the reoxidation of **IM7** occurs through associative interchange with PhNNPh (**TS5** $\Delta G^{\ddagger}$ = 17.5 or 14.9 kcal/mol) or through pyrrole dissociation to free/solvated Ti^{II} (**IM10** ΔG = 32.1 or 9.9 kcal/mol). Given the abundance of potential π-acceptors in these reactions (alkyne, azobenzene, solvent), an associative interchange mechanism with some stabilizing ligand is certainly plausible.

Why is reductive elimination so facile? First, backbonding of the resultant low valent Ti^{II} species into the pyrrole product π* orbitals stabilizes **IM7**. This backbonding can be seen in the elongation (~1.45 Å *vs* ~1.38 Å in *N*-Ph pyrrole[43]) of the C-N bonds of the calculated structure of **IM7** (Figure 7A), as well as in NICS and NBO analysis. Synergistic backbonding with π-acceptor products provides a thermodynamic rationale for why reductive elimination is favorable, similar to how redox noninnocent ligands cooperatively attenuate metal electron density. Formation of 2-electron π-backbonded species may also help attenuate competitive radical Ti^{III} processes; indeed, significant work on the reactivity of π-backbonded "masked" Ti^{II} fragments has been reported.[28,44,45]

The second factor contributing to facile reductive elimination is that C-N coupling proceeds through a π electrocyclic mechanism rather than Ti-N/Ti-C σ-bond coupling. This hypothesis emerged from intrinsic bond orbital (IBO) analysis[46] of reductive elimination (Figure 7, B and C), where one can observe the π-to-σ transformation seen in electrocyclic reactions: the N-Ti π bond in **IM6** (blue) rotates and attacks C4 to form the new C-N bond, while the π bonds on the metallacycle (orange and green) shift to localize on C1, C2, and C3. Concurrent with C-N bond formation, the Ti-C and Ti-N σ-bonding orbitals rotate perpendicular to the forming pyrrole plane and form a π-backbond with Ti. The overall transformation[47] is similar to an aza-Nazarov cyclization.[48,49]

Electrocyclic reductive elimination kinetically enables much of the Ti redox catalysis herein; further, it may play an important role in reactions across the periodic table. For example, pericyclic redox mechanisms have been demonstrated in asymmetric Tsuji allylic alkylation,[50] P^{III}/P^{V} reductive transposition,[51] and lanthanide-promoted pyrimidine formation.[52]

Studies into well-behaved examples of electrocyclic reductive elimination will be important for better understanding the requirements for these transformations. Fortier recently reported a reversible thiophene C-S oxidative addition/reductive elimination sequence from arene-masked Ti^{II} complex **9** (Figure 8).[53] DFT calculations of oxidative addition show Ti backdonation into the thiophene π* orbital prior to bond torsion and C-S bond cleavage, similar to the reverse C-N bond formation (Figure 7). Photoexcitation of **10** results in a ligand-to-metal charge transfer, which triggers electrocyclic ring-closure and regeneration of thiophene and **9**. Unlike pyrrole/py_3TiCl_2(NPh) catalysis where reductive elimination is thermodynamically favored, thiophene oxidative addition is favored with **9**. This difference

could be a result of ligand effects (electron-rich and bulky in **9**, electron-deficient in $py_3TiCl_2(NPh)$), or a reflection of the aromatic stabilization of pyrrole relative to thiophene.

CATALYST DEVELOPMENT

Discovery of Catalysts.

Given the initial substoichiometric reactions with **2** (Figure 3) and the relationship of the [2+2+1] reaction with alkyne hydroamination, we tested many highly active hydroamination catalysts for [2+2+1] reactivity. Disappointingly, most complexes exhibited little or no catalytic activity, although several stoichiometrically generate pyrrole and cyclotrimerize alkynes.[54]

Instead, simple electron-deficient Ti halides[55] remain the most effective catalysts (Figure 9A), with more electron-deficient[56] **13** catalyzing the formation of **1j** the fastest compared to **12** and **11** (this trend holds across most alkynes, although **13** competitively trimerizes terminal alkynes). The rationale for this activity is that rate-determining alkyne binding and insertion into **TS3** (Figure 4) relies on dative donation of the alkyne **π**-bond to Ti, which will be stronger for electron-deficient complexes. Further, **TS3** is sterically encumbered (forming **IM6** from **IM4** requires 3 *fac*-binding sites), so lower-coordinate complexes insert more readily—for example, removal of excess pyridine (**14** vs **11**) significantly increases reaction rate, indicating strong pyridine inhibition.

ETM complexes are often unfairly disregarded as impractical owing to their purported air sensitivity. However, Ti halide imido catalysts can easily be made *in situ* from the air-stable precursor $TiCl_4(THF)_2$ through reduction by Zn powder (Figure 9B).[57] Here, single-electron reduction to Ti^{III} is enough to generate a Ti imido through disproportionation with azobenzene. This *in situ* protocol can be used to carry out virtually all of the reactions reported in this *Account* on the benchtop, typically with only mild impacts on yield.

Regioselective Catalyst Design.

A limitation of initial [2+2+1] pyrrole syntheses was that reactions with unsymmetrical alkynes (*e.g.* **1e**-**1h**, Figure 2B) were not regioselective. Thus, regiocontrol was an initial goal of catalyst development. Early challenges in rational design led us to attempt higher-throughput reaction screens from *in situ* reaction of $[TiCl_2(NPh)]_n$[58] with L donors, forming "$L_nTiCl_2(NPh)$" (Figure 10A). From these *in situ* studies and follow-ups with pre-formed "$L_nTiCl_2(NPh)$," it appeared that substituted pyridine ligands could have subtle effects on the regioselectivity of phenylpropyne homocoupling—for example, 2,6-lutidine (**17**) was moderately selective (~2:1 against other regioisomers) for 2,5-Me_2-1,3,4-Ph_3-1*H*-pyrrole **1f"** (Figure 10B).

Using a new computational/statistical prediction tool, iterative supervised principal component analysis (ISPCA),[59] led to the prediction (and experimental confirmation) that complexes of sterically encumbered electron-rich pyridines (**18**) would be highly selective for **1f"**. This selectivity was rationalized as a result of (1) steric control of 2nd alkyne insertion ($\Delta\Delta G^{\ddagger}$ (**TS3**-**TS3"**) = 3.4–3.8 kcal/mol) imparted by the pyridine ligand;

and (2) strongly donating pyridines disfavoring the dissociation equilibria to non-ligated (nonselective) species (Figure 10C).

Other Catalysts.

Tsurugi and Mashima found that V-based precatalysts, in combination with $PhN(SiMe_3)_2$ **19** (used to make M=NPh *in situ*) are competent for [2+2+1] coupling (Figure 11A).[60] Other metals ($NbCl_5$, $TaCl_5$, $MoCl_5$, WCl_6) in combination with **19** also yielded pyrrole with lower yields. These observations indicate that catalytic oxidative amination manifolds may be broadly accessible with ETMs.[61]

The $VCl_3(THF)_3$/$PhN(SiMe_3)_2$ scope (Figure 11B) is similar to that catalyzed by $[py_2TiCl_2(NPh)]_2$, although unsymmetrical alkynes (**1f**) had different selectivities (notably, no formation of **1f'**). Additionally, there were several mechanistic differences (Figure 11C): first, the active species is a *bis*(imido) **IM12**.[62] Second, the rate law is 2nd order in $[VCl_3(THF)_3]$ and 1st order in [5-decyne] and [azobenzene], indicating that bimetallic reoxidation of **IM11** (V^{III}) to **IM12** (V^{V}) is kinetically relevant and that **IM11** may be the resting state, consistent with the higher oxidation potential of V^{III} compared to Ti^{II}.

MULTICOMPONENT REACTIONS WITH ALKYNES

A key observation from mechanistic studies of Ti-catalyzed pyrrole synthesis[2] was that alkyne engagement occurred in 2 distinct steps, opening the door for potential multicomponent reactions through selective reactivity at each step. Accordingly, significant progress has been made in multicomponent oxidative aminofunctionalization of alkynes, where the azatitanacyclobutene [2+2] cycloadduct can be intercepted by a variety of other substrates.

[2+2+1] Alkyne Heterocouplings: Functionalized Pyrrole Synthesis.

In an effort to further exert regiocontrol over [2+2+1] pyrrole synthesis, we envisioned that heterocoupling of two stereoelectronically differentiated alkynes may lead to better regioselectivity, assuming the *chemo*selectivity of alkyne coupling could be controlled.

We had earlier found that 1-phenyl-2-trimethylsilylacetylene (**20a**) was unreactive in [2+2+1] pyrrole synthesis, as it is incapable of facile [2+2] cycloaddition with $py_3TiCl_2(NPh)$. Thus, TMS-substituted alkynes were targeted as selective 2nd insertion partners in a [2+2+1] heterocoupling manifold—and found to be remarkably efficient and selective alkynes for cross-selective pyrrole formation (Figure 12A).[3] This reaction was demonstrated with many TMS-substituted alkynes, including aryl (*e.g.* **21a**, **21b**), conjugated (**21c**), alkyl (**21d**), coupled to PhCCMe and other internal alkynes (*e.g.* **21e-g**) (Figure 12B). This modularity allows for direct synthesis of regioisomeric pyrroles such as **21b** and **21f**. Additional selective heterocouplings have subsequently been reported with boryl and stannyl alkynes, yielding 2-boryl- or 2-stannyl-substituted pyrroles.[63]

Regiocontrol for both the TMS-substituted alkyne and the partner alkyne is a function of electronic demands. In [2+2] cycloaddition, **TS2/IM5** better stabilize building ∂^+ on the $C\text{-}CH_3$ rather than on C-Ph in **TS2'/IM5'** ($\Delta\Delta G^{\ddagger}$ = −1.5 kcal/mol, ΔG = −4.7 kcal/mol)

(Figure 12C). For 2nd alkyne insertion, the silyl group can hyperconjugate to stabilize partial positive charge buildup[64] on C_β during **TS6**, and the resultant Ti-C_α-$SiMe_3$ bond is stronger than the alternative Ti-C_α-R bond. Similar effects have been observed in other group 4 insertions[65,66] and have been used to affect regioselective reductive couplings.[67]

The chemoselectivity of 2nd alkyne insertion is driven by alkyne coordination. Here, electron-rich alkynes such as TMS-protected alkynes will bind more strongly to Ti^{IV}, since there is no possibility for backdonation from Ti^{IV}. A bonus effect is that TMS-alkyne reactions are significantly faster ($t \leq 1.5$ h), and run at lower temperatures (≤ 90 °C) compared to homocoupling[1] of alkynes. These advantages are also an effect of the electron-rich TMS-protected alkyne: since 2nd insertion is rate-limiting, facile alkyne coordination likely leads to faster insertion.

During investigation of the alkyne heterocoupling scope, 2-pyridyl pyrrole **21h'** was found to be the major product from **20h**, rather than the expected 3-substituted **21h**. This is a result of pyridine coordination (Figure 13, **TS6'**), which directs the TMS-alkyne insertion to occur with opposite regioselectivity. We next developed methods to exploit this directing effect, demonstrating directed insertion with 9 functional groups.[68] The directing effect can be tuned by changing the catalyst: while 2-py-substituted **20h** results in high **21h'** selectivity with $[py_2TiCl_2(NPh)]_2$, the weaker Lewis base *o*-OMe **20i** is completely unselective. However, moving to the more Lewis acidic catalyst $(THF)_3TiI_2(NPh)$ results in highly 2-selective coupling of **20i** owing to the stronger Lewis acid-base interaction. On the other hand, more Lewis basic **20h** results in no catalysis with $(THF)_3TiI_2(NPh)$ due to inhibition by pyridine coordination.

Installation of silyl, boryl, and stannyl groups onto the pyrrole provides a platform for post-functionalizations such as electrophilic aromatic substitutions (**22**) or cross-coupling reactions (**25**) (Figure 14A/B). **21** and **24** are hydrolytically unstable and must be further transformed *in situ*, while stable stannyl pyrroles can be isolated. These methods can be telescoped into multistep syntheses, as demonstrated in a formal synthesis of Lamellarin R^3,[69] (**26**) and the synthesis of a 1,5-biaryl pyrrole EP_1 receptor antagonist[68,70] **27** (Figure 14C).

Ultimately, Ti-catalyzed [2+2+1] protocols are extremely modular/flexible strategies for the synthesis of highly substituted and/or electron-rich *N*-aryl pyrroles. They are complementary to condensation (Paal-Knorr, Lewis acid-catalyzed, *etc.*) or cycloisomerization strategies, each of which typically perform best for electron-deficient pyrroles (*e.g.* acyl-substituted) and often have specific regiochemical limitations.[71] A current limitation of Ti-catalyzed protocols is the inability to access *N*-protected or *N*-H pyrroles arising from several factors: (1) incompatibility of the Ti complexes with oxygenated functional groups (Ts, CO_2R, *etc.*); (2) thermally-triggered radical decomposition of R-NN-R ($R \neq Ar$) diazenes; and (3) substitution reactivity of Ti-X with R_3SiN_3 that generates Ti-N_3 complexes. However, with intentional catalyst and methods development it should be possible to overcome these challenges in the future.

Alkyne + Alkene Coupling: Oxidative Alkyne Carboamination.

Unlike alkynes, most alkenes do not readily undergo [2+2] cycloaddition with Ti imidos. Thus, alkenes can also potentially be incorporated into multicomponent oxidative amination reactions through selective 2nd insertion of the alkene. Reactions of tethered enynes (**28**) catalyzed by $[py_2TiCl_2(NPh)]_2$ resulted in the formation of either α,β-unsaturated imines (**29**) or cyclopropylimines (**30**), the products of oxidative alkyne carboamination (Figure 15A).[72] Both products are formed from azatitanacyclohexadiene **IM15** (Figure 15C) which then undergoes either (1) pericyclic C_α-C_γ reductive coupling (**TS7**) to form **IM16** (then **30**) or (2) β-H elimination to **IM17**, followed by reductive elimination to form **29**. C-N reductive elimination to 2,3-dihydropyrroles is not observed, presumably because C_α-C_β saturation in **IM15** prevents electrocyclic ring closure.

Product selectivity (**29**:**30**) is very sensitive to the starting enyne structure (Figure 15B). For example, propylene-linked **28a** is selective for α,β-unsaturated imine **29a** (85:15), while butylene-linked **28d** is unselective (49:51). β-deuterated **28b** is less selective than **28a** (53:47) as the kinetic isotope effect makes β-D elimination less favorable. β-Me substituted **28e**, which cannot undergo β-H elimination, yields exclusively **30e**. Internal tethered enynes **28c** and **28f** yield exclusively α,β-unsaturated **29c** and **29f**.

The mechanism for **IM15** formation is similar to previous examples.[2] However, the mechanism for β-H elimination and reductive elimination from **IM17** reveals interesting new reactivity. Computational analysis by Wang[73] indicates that reductive elimination from **IM17** likely occurs via reinsertion of Ti-H into either C_α (**IM18**) followed by associative interchange with azobenzene to liberate **29** and regenerate **IM4**.

Evidence for a Ti-H reinsertion mechanism can be seen in *inter*molecular reactions (Figure 16A). Oxidative carboamination of 3-hexyne or 2-butyne with allylanisole (**31**) and azobenzene results in the formation of unconjugated β,γ-unsaturated imine **32**. Since **14** is no longer bicyclic and thus has more rotational degrees of freedom, Ti-H insertion into the remote C_γ position can occur, leading to **IM18'** (Figure 16B). Unfortunately, product selectivity in Ti-catalyzed oxidative carboamination remains under subtle substrate control and the specific control elements remain unclear—for example, switching from 2-butyne to 3-hexyne completely inverts the selectivity (15:85 to 71:29) in reactions with **31**.

Related redox-neutral group 4-catalyzed alkyne carboaminations were reported by Bergman[74] and Mindiola[75] (Figure 17). In these examples, insertion of diaryl aldimines (**33**) into Ti/Zr azametallacyclobutenes (**IM19**) led to diazametallacyclohexenes (**IM20**), which undergo *retro*-[4+2] sequences to liberate α,β-unsaturated imines **34** and regenerate the Ti/Zr imido. Although limited to aryl aldimines and alkynes, further investigation of this reaction class is warranted given increased interest in carboamination catalysis across the periodic table.[76–78]

Alkyne + Nitrile Coupling: Pyrazole Synthesis.

Pyrazoles are pharmaceutically important heterocycles that are commonly made *via* Knorr-like condensation of hydrazines onto 1,3-diketones, or via 1,3-dipolar cycloaddition of

hydrazones with alkynes. Regioselectivity issues in these reactions, along with potential safety concerns around hydrazines, provide a compelling rationale to develop alternative synthetic routes.

Nitriles were explored as potential 2nd insertion partners in an effort to extend Ti redox catalysis to pyrazole synthesis. Livinghouse previously demonstrated intermolecular capture of an azatitanacyclobutene (generated by intramolecular [2+2] cycloaddition of **37**) by isobutyronitrile, leading to diazatitanacyclohexadiene **IM21** (Figure 18A).[35] Thus, the basic coupling framework for [2+2+1] pyrazole synthesis was already in place, although this reaction would require N-N reductive elimination from the diazatitanacycle. Examples of organometallic N-N bond-forming methods are extremely limited;[79,80] however, since C-N reductive elimination in the related pyrrole synthesis occurs *via* electrocyclization, we hypothesized that a similar mechanism could allow access to this unusual N-N coupling.

Unfortunately, attempts at Ti-imido-catalyzed [2+2+1] pyrazole synthesis have mostly failed. Diazatitanacycle **IM22** (Figure 18B) is too stable to undergo facile reductive elimination; compared to **IM6**, the introduction of a 2nd strong Ti-N bond in **IM22** results in significant stabilization.

However, the stability of diazatitanacycle **IM22** meant that they could be synthesized *in situ* (or isolated) from alkynes, nitriles, and imidos and subjected to further reactivity. Although **IM22** is Ti^{IV}, we hypothesized that *ligand*-based oxidation may promote electrocyclic N-N bond formation. Several oxidants provide facile N-N coupling of **IM22**, with 2 equiv. TEMPO performing best. This protocol was then developed into a 1-pot, 2-step multicomponent cyclization/oxidation sequence for the synthesis of a diverse array of pyrazoles (**39**) (Figure 18B).[4]

Pyrazole formation requires 2 oxidation equivalents for full conversion, although N-N coupling could occur through three oxidation states: the “default” oxidation state **IM22**, 1-electron oxidized **IM23**, or 2-electron oxidized **IM24** (Figure 19A) Previously, we had shown that Ti^{II} synthons could ring-open 2*H*-azirines,[81] and thus hypothesized that ring-opening of 2-imino-2*H*-azirine **40** (isomer of pyrazole **41**) by Ti^{II}, Ti^{III}, or Ti^{IV} would lead to diazatitanacycles with oxidation states analogous to **IM22**, **IM23**, or **IM24**, respectively, such that we could probe the oxidation state coupling question. Reaction of **40** with Cp_2Ti(BTMSA) led to stable **IM22**, reaction with $TiCl_4$ led to full conversion to **40**, and reaction with $TiCl_3(THF)_3$ led to a 50:50 mixture of **40** and **IM22** (Figure 19B).[4] These stoichiometric reactions indicate that N-N coupling occurs *via* **IM24**, which can be accessed either through direct 2-electron oxidation or *via* redox disproportionation of **IM23** (likely the case for TEMPO).

Alkyne Diimination.

Since **IM22** underwent electrocyclic N-N coupling upon oxidation, we next aimed to explore the potential for **IM22** to undergo other cycloaddition reactions. We envisioned that **IM22** could serve as an electron-rich diene in [4+2] cycloaddition reactions with polar dienophiles.[82] Reactions of *C*-nitrosos (**43**) with preformed diazatitanacycle **42** were explored, resulting in rapid, near-quantitative formation of α-diimines **44**, along with

expulsion of *p*-tolunitrile (Figure 20A). Interestingly, the yields of α-diimines are consistent irrespective of *C*-nitroso substitution—perhaps a reflection of the strong driving force of Ti-O formation.

Based on these results, a 2-step, 1-pot oxidative alkyne diimination method was developed (Figure 20B).[82] As in the multicomponent pyrazole syntheses, the α-diimine yields are determined by the efficiency of forming diazatitanacycle **IM25** and use of excess MeCN as the nitrile component significantly improves metallacycle formation. This alkyne diimination provides facile and modular access to fully unsymmetric α-diimines (**45**), which are often impossible to make *via* stepwise condensation (which is reversible). Regioisomeric series of α-diimines can be easily constructed by swapping substituents on the various components, for example in **45a**-**45c** (Figure 20C).

Computational analysis indicates that this reaction proceeds via [4+2] cycloaddition of the *C*-nitroso across **IM25** to form **IM26**, followed by a *retro*-[4+2] cycloaddition that expels nitrile and produces **IM27** (Figure 20B). From **IM27**, N-O bond cleavage *via* α-N elimination (**IM28**) generates a diimine-coordinated Ti oxo species which liberates **45.**

This two-step reaction sequence is required for productive α-diimine formation because *C*-nitrosos undergo direct [2+2] cycloaddition with Ti≡NR to produce Ti=O and RN=NR. Thus, the nitrile component serves as a promoter in the reaction, first forming the key intermediate **IM25** and then being expelled prior to product formation.

OTHER OXIDATIVE AMINATION REACTIONS

Although group 4-catalyzed oxidative amination reactions have primarily been explored with alkynes, other types of reactive functional groups are also capable of undergoing catalytic oxidation. There is a wealth of examples of stoichiometric reactions of unsaturated functional groups with group 4 metal imido complexes, which serve as the inspiration for development of new catalytic protocols.

Ring-Opening Oxidative Amination of Methylenecyclopropanes.

Strained exocyclic double bonds, like those in methylenecyclopropanes (MCPs), undergo [2+2] cycloadditions with Ti imidos. Eisen demonstrated ring-opening hydroamination[83,84] of 2-aryl MCPs (**46**), suggesting that ring strain confers “sp-like” character onto the alkene (Figure 21A) and promotes cycloaddition. After [2+2] cycloaddition, β-C elimination and aminolysis generates **47**.

Ti-catalyzed ring-opening oxidative aminations of MCPs (**48**) with PhNNPh are also possible (Figure 21B), yielding unusual α-methylene imines (**49**) or cyclic α,β-unsaturated imines (**50**).[85] These reactions follow a similar mechanism to MCP hydroamination, however here **IM30** undergoes β-H elimination to **IM31** (Figure 21C). From **IM31**, hydride re-insertion (similar in catalytic alkyne carboamination, Figure 16B) results in formation of the backbonded α,β-unsaturated imine intermediate **IM32**, which can undergo associative exchange with azobenzene to close the catalytic cycle. The regioselectivity of ring-opening is opposite that observed in Eisen’s hydroamination[83,84] and is a substituent effect: aryl

MCPs undergo scission between C_{aryl} and $C{=}CH_2$, while alkyl MCPs undergo scission between $C_{unsubst}$ and $C{=}CH_2$.

Nitrene Isocyanation and Carbonylation.

In a seminal example from Heyduk, redox-noninnocent[86] Zr complex **51** catalyzed transfer of nitrenes from alkyl azides to isocyanides, forming unsymmetrical carbodiimides (**52**) (Figure 22A).[87] Isocyanide insertion into group 4 metal imidos is well-known, but the resultant η^2-carbodiimides are often unreactive due to strong backbonding. With **51**, catalytic turnover can be achieved because the NNN ligand in **IM35** can accept the pair of electrons that were previously backbonding into the η^2-carbodiimide and render the carbodiimide labile. Similarly, Wolczanski reported catalytic nitrene carbonylation using a Ti complex of a redox noninnocent diamide, diimine ligand.[88]

We hypothesized isocyanide imination with simple Ti imidos using azobenzene or organoazides as the nitrene source may be possible (Figure 22B), since azobenzene is a strong π-acceptor and could serve the same role as Heyduk's/Wolczanski's redox-noninnocent ligands. A small screen of Ti imido halides showed that Cl, Br, and I derivatives (**11–14**, from Figure 9) were competent catalysts for imination of ^{t}BuNC with PhNNPh,[89] with Br complex **53** deemed the best balance between reactivity and catalyst cost. Reactions proceeded effectively with ^{t}BuNC yielding unsymmetric **54**, while 2,6-Me_2-PhNC and CyNC were poorly reactive owing to product inhibition. Catalysis with these latter substrates could be accomplished by switching to a bulkier nitrene source such as AdN_3. DFT calculations support an azobenzene-bound mechanism, wherein the carbodiimide product release (**IM38**) is triggered by electron transfer from the η^2-carbodiimide to azobenzene.

CONCLUSION

In summary, this *Account* discusses the surprisingly versatile 2-electron redox chemistry of Ti imido complexes, driven by substrates and products that can π-backbond effectively at key states during catalysis. Fundamental mechanistic studies of Ti redox catalysis in the context of [2+2+1] pyrrole synthesis have led to new strategies for the synthesis of important 5-membered aromatic heterocycles, as well as other aminated products.

Looking forward, there still remains significant opportunity to exploit the fundamental reactivity of early transition metal complexes for redox catalysis—which, importantly, will likely have orthogonal selectivity and functional group tolerance when compared to late transition metal-catalyzed methods. A significant ongoing challenge will be in uncovering new strategies for catalytic turnover for cases where π-backbonding does not provide enough thermodynamic stabilization for metal reduction, or in cases where pericyclic reactivity may not be possible. Here, drawing inspiration from modern catalytic methods (electrochemistry, photoredox catalysis, *etc.*) that have not been employed frequently with early transition metals will be critical for opening new doors in catalytic oxidative reactions.

ACKNOWLEDGMENT

To all of the students, postdocs, and collaborators in the group over the past eight years: thank you for all of your hard work, creativity, perseverance, and teamwork. The success of all of the projects reported herein is a reflection

of your collective strengths. This work has been generously supported by the University of Minnesota, the NIH (R35GM119457), and the Alfred P. Sloan Foundation.

Funding Sources

No competing financial interests have been declared.

Biographical Information

Ian A Tonks is the Lloyd H. Reyerson Professor in the Department of Chemistry at the University of Minnesota – Twin Cities, and Associate Editor for the ACS journal *Organometallics*. He received his B.A. from Columbia University, followed by his Ph.D. from the California Institute of Technology, and postdoctoral studies at the University of Wisconsin – Madison. His research program is focused on earth abundant catalysis and developing new strategies for CO_2 utilization in polymer synthesis.

REFERENCES

1. Gilbert ZW; Hue RJ; Tonks IA Catalytic Formal [2+2+1] Synthesis of Pyrroles from Alkynes and Diazenes via Ti^{II}/Ti^{IV} Redox Catalysis. Nature Chemistry 2016, 8, 63–68.
2. Davis-Gilbert ZW; Wen X; Goodpaster JD; Tonks IA Mechanism of Ti-Catalyzed Oxidative Nitrene Transfer in [2+2+1] Pyrrole Synthesis. J. Am. Chem. Soc. 2018, 140, 7267–7281. [PubMed: 29763560]
3. Chiu H-C; Tonks IA Trialkylsilyl-Protected Alkynes as Selective Cross Coupling Partners in Ti-Catalyzed [2+2+1] Pyrrole Synthesis. Angew. Chem. Int. Ed. 2018, 57, 6090–6094.
4. Pearce AJ; Harkins RP; Reiner BR; Wotal AC; Dunscomb RJ; Tonks IA Multicomponent Pyrazole Synthesis from Alkynes, Nitriles, and Titanium Imido Complexes *via* Oxidatively-Induced N-N Bond Coupling. J. Am. Chem. Soc. 2020, 142, 4390. [PubMed: 32043879]
5. Vitaku E; Smith DT; Njardarson JT Analysis of the Structural Diversity, Substitution Patterns and Frequency of Nitrogen Heterocycles among US FDA Approved Pharmaceuticals. J. Med. Chem. 2014, 57, 10257–10274 [PubMed: 25255204]
6. Ertl P; Altmann E; McKenna JM The Most Common Functional Groups in Bioactive Molecules and How Their Popularity Has Evolved over Time. J. Med. Chem. 2020, 63, 8408–8418. [PubMed: 32663408]
7. Huang L; Arndt M; Gooßen K; Heydt H; Gooßen LJ Late Transition Metal-Catalyzed Hydroamination and Hydroamidation. Chem. Rev. 2015, 115, 2596–2697. [PubMed: 25721762]
8. Müller TE; Hultzsch KC; Yus M; Foubelo F; Tada M Hydroamination: Direct Addition of Amines to Alkenes and Alkynes. Chem. Rev. 2008, 108, 3795–3892. [PubMed: 18729420]
9. Degennaro L; Trinchera P; Luisi R Recent Advances in the Stereoselective Synthesis of Aziridines. Chem. Rev. 2014, 114, 7881–7929. [PubMed: 24823261]
10. Park Y; Kim Y; Chang S Transition Metal-Catalyzed C-H Amination: Scope, Mechanism, and Applications. Chem. Rev. 2017, 117, 9247–9301. [PubMed: 28051855]
11. Roglans A; Pla-Quintana A; Solà M Mechanistic Studies of Transition-Metal-Catalyzed [2+2+2] Cycloaddition Reactions. Chem. Rev. 2021, 121, 1894–1979. [PubMed: 32786426]
12. Nugent WA; Mayer JM Metal-Ligand Multiple Bonds: The Chemistry of Transition Metal Complexes Containing Oxo, Nitrido, Imido, Alkylidene, or Alkylidyne Ligands. (Wiley, 1988).
13. Hunt AJ; Farmer TJ; Clark JH in Element Recovery and Sustainability (ed. Hunt AJ) 1–8 (Royal Society of Chemistry, 2013).
14. Schafer L; Hill M; Tonks IA Organometallic Complexes of Electrophilic Elements for Selective Synthesis. Organometallics 2018, 37, 4311–4312.
15. McCallum T; Wu X; Lin S Recent Advances in Titanium Radical Redox Catalysis. J. Org. Chem. 2019, 84, 14369–14380. [PubMed: 31647872]

16. Rodríguez MC; García IR; Maecker RNR; Morales LP; Oltra JE; Martínez AR Cp_2TiCl: An Ideal Reagent for Green Chemistry? Org. Process Res. Dev. 2017, 21, 911–923.
17. Yao C; Dahmen T; Gansäuer A; Norton J Anti-Markovnikov Alcohols via Epoxide Hydrogenation through Cooperative Catalysis. Science 2019, 364, 764–767. [PubMed: 31123133]
18. Gansäuer A From Enantioselective to Regiodivergent Epoxide Opening and Radical Arylation – Useful or Just Interesting? Synlett 2021, 32, 447–456.
19. Negishi E Controlled Carbometallation as a New Tool for Carbon-Carbon Bond Formation and its Application to Cyclization. Acc. Chem. Res. 1987, 20, 65–72.
20. Beaumier EP; Pearce AJ; See XY; Tonks IA Modern Applications of Low Valent Early Transition Metals in Synthesis and Catalysis. Nat. Rev. Chem. 2019, 3, 15–34. [PubMed: 30989127]
21. Lyaskovskyy V; de Bruin B Redox Non-Innocent Ligands: Versatile New Tools to Control Catalytic Reactions. ACS Catal. 2012, 2, 270–279.
22. Kawakita K; Kakiuchi Y; Tsurugi H; Mashima K; Parker B; Arnold J; Tonks IA Reactivity of Terminal Imido Complexes of Group 4–6 Metals: Stoichiometric and Catalytic Reactions Involving Cycloaddition with Unsaturated Organic Molecules. Coord. Chem. Rev. 2020, 407, 213118. [PubMed: 32863399]
23. Tonks IA; Meier JC; Bercaw JE Alkyne Hydroamination and Trimerization with Titanium Bis(phenolate)pyridine Complexes: Evidence for Low-Valent Titanium Intermediates and Synthesis of an Ethylene Adduct of Titanium(II). Organometallics 2013, 32, 3451–3457.
24. Pearce AJ; See XY; Tonks IA Oxidative Nitrene Transfer from Azides to Alkynes via Ti(II)/Ti(IV) Redox Catalysis: Formal [2+2+1] Synthesis of Pyrroles. Chem. Commun. 2018, 54, 6891–6894.
25. Burés J Variable Time Normalization Analysis: General Graphical Elucidation of Reaction Orders from Concentration Profiles. Angew. Chem. Int. Ed. 2016, 55, 16084–16087.
26. Guo J; Deng X; Song C; Lu Y; Qu S; Dang Y; Wang Z-X Differences Between the Elimination of Early and Late Transition Metals: DFT Mechanistic Insights into the Titanium-Catalyzed Synthesis of Pyrroles from Alkynes and Diazenes. Chem. Sci. 2017, 8, 2413–2425. [PubMed: 28451348]
27. Duchateau R; Williams AJ; Gambarotta S; Chiang MY Carbon-Carbon Double-Bond Formation in the Intermolecular Acetonitrile Reductive Coupling Promoted by a Mononuclear Titanium(II) Compound. Preparation and Characterization of Two Titanium(IV) Imido Derivatives. Inorg. Chem. 1991, 30, 4863–4866.
28. Hill JE; Profilet RD; Fanwick PE; Rothwell IP Synthesis, Structure, and Reactivity of Aryloxo(imido)titanium Complexes. Angew. Chem. Int. Ed. 1990, 29, 664–665.
29. Gray SD; Thorman JL; Adamian VA; Kadish KM; Woo LK Synthesis, Electrochemistry, and Imido Transfer Reactions of (TTP)Ti(η2-PhN=NPh). Inorg. Chem. 1998, 37, 1–4. [PubMed: 11670252]
30. Pohlki F; Doye S The Mechanism of the $[Cp_2TiMe_2]$-Catalyzed Intermolecular Hydroamination of Alkynes. Angew. Chem. Int. Ed. 2001, 40, 2305–2308.
31. Straub BF; Bergman RG The Mechanism of Hydroamination of Allenes, Alkynes, and Alkenes Catalyzed by Cyclopentadienyl-Imido Complexes: A Density Functional Study. Angew. Chem. Int. Ed. 2001, 40, 4632–4635.
32. Walsh PJ The Synthesis and Chemistry of Organozirconocene Complexes Containing Zirconium-Nitrogen Double and Single Bonds. Ph.D. Thesis, University of California – Berkeley, Berkeley, CA, 1990.
33. Vujkovic N; Ward BD; Maisse-François A; Wadepohl H; Mountford P; Gade LH Imido-Alkyne Coupling in Titanium Complexes: New Insights into the Alkyne Hydroamination Reaction. Organometallics 2007, 26, 5522–5534.
34. Lokare KS; Ciszewski JT; Odom AL Group-6 Imido Activation by a Ring-Strained Alkyne. Organometallics 2004, 23, 5386–5388.
35. McGrane PL; Jensen M; Livinghouse T Intramolecular [2+2] cycloadditions of Group IV metal-imido complexes. Applications to the synthesis of dihydropyrrole and tetrahydropyridine derivatives. J. Am. Chem. Soc. 1992, 114, 5459–5460.
36. Hanna TA; Baranger AM; Bergman RG Reactivity of Zirconocene Azametallacyclobutenes: Insertion of Aldehydes, Carbon Monoxide, and Formation of a,b-Unsaturated Imines. Formation

and Trapping of [Cp_2Zr=O] in a [4+2] Retrocycloaddition. J. Org. Chem. 1996, 61, 4532–4541. [PubMed: 11667377]

37. Ruck RT; Bergman RG Reactions of Imines with Azazirconacyclobutenes and Generation of Electron-Deficient Imidozirconocene Complexes. Organometallics 2004, 23, 2231–2233. [PubMed: 16508694]
38. Odom AL; McDaniel TJ Titanium-Catalyzed Multicomponent Couplings: Efficient One-Pot Syntheses of Nitrogen Heterocycles. Acc. Chem. Res., 2015, 48, 2822–2833. [PubMed: 26295382]
39. Cao C; Shi Y; Odom AL A Titanium-Catalyzed 3-Component Coupling to Generate α,β-Unsaturated β-Iminoamines. J. Am. Chem. Soc 2003, 125, 2880–2881. [PubMed: 12617647]
40. Cloke FGN; Hitchcock PB; Nixon JF; Wilson DJ; Tabellion F; Fischbeck U; Preuss F; Regitz M Synthetic, structural and theoretical studies on new aromatic 1,2,4-azadiphosphole ring systems: crystal and molecular structure of P_2C_2But2NPh. Chem. Commun. 1999, 2363–2364.
41. Negishi E; Takahashi T Patterns of Stoichiometric and Catalytic Reactions of Organozirconium and Related Complexes of Synthetic Interest. Acc. Chem. Res. 1994, 27, 124–130.
42. Siebeneicher H; Doye S Dimethyltitanocene Cp_2TiMe_2: A Useful Reagent for C–C and C–N Bond Formation J. Prakt. Chem. 2000, 342, 102–106.
43. Meindl K; Henn J; Kocher N; Leusser D; Zachariasse KA; Sheldrick GM; Koritsansky T; Stalke D Experimental Charge Density Studies of Disordered *N*-Phenylpyrrole and N-(4-Fluorophenyl)pyrrole. J. Phys. Chem. A 2009, 113, 9684–9691. [PubMed: 19673504]
44. Thorn MG; Hill JE; Waratuke SA; Johnson ES; Fanwick PE; Rothwell IP J. Am. Chem. Soc. 1997, 119, 8630–8641.
45. Rosenthal U Update for Reactions of Group 4 Metallocene Bis(trimethylsilyl)acetylene Complexes: A Never-Ending Story? Organometallics 2020, 39, 4403–4414.
46. Knizia G; Klein JEMN Electron flow in reaction mechanisms --- revealed from first principles Angew. Chem. Int. Ed. 2015, 54, 5518–5522.
47. This mechanism may be involved in other pyrrole syn-theses. See: (A)Matsui K; Shibuya M; Yamamoto Y Synthesis of pyrroles via ruthenium-catalyzed nitrogen-transfer [2 + 2+1] cycloaddition of α,ω-diynes using sulfoximines as nitrene surrogates. Commun. Chem. 2018, 1, 21.(B)Haut F-L; Feichtinger NJ; Plangger I; Wein LA; Müller M; Streit T-N; Wurst K; Podewitz M; Magauer T Synthesis of Pyrroles via Consecutive 6π-Electrocyclization/Ring Contraction of Sulfilimines. J. Am. Chem. Soc. 2021 143, 9002–9008. [PubMed: 34106724]
48. Vinogradov MG; Turova OV; Zlotin SG Nazarov reaction: current trends and recent advances in the synthesis of natural compounds and their analogs. Org. Biomol. Chem. 2017, 15, 8245–8269. [PubMed: 28960012]
49. Dieker J; Frölich R; Würthwein E-U Substituted 3-Hydroxypyrroles from 1-Azapenta-1,4-dien-3-ones: The Aza-Nazarov Reaction – Synthesis and Quantum Chemical Calculations. Eur. J. Org. Chem. 2006, 5339–5356.
50. Cusumano AQ; Goddard III WA; Stoltz BM The Transition Metal Catalyzed [π2s + π2s + σ2s + σ2s] Pericyclic Reaction: Woodward–Hoffmann Rules, Aromaticity, and Electron Flow. J. Am. Chem. Soc. 2020, 142, 19033–19039. [PubMed: 33107727]
51. Reichl KD; Dunn NL; Fastuca NJ; Radosevich AT Biphilic Organophosphorus Catalysis: Regioselective Reductive Transposition of Allylic Bromides via P^{III}/P^{V} Redox Cycling. J. Am. Chem. Soc. 2015, 137, 5292–5295. [PubMed: 25874950]
52. Lv Z-J; Chai Z; Zhu M; Wei J; Zhang W-X Selective Coupling of Lanthanide Metallacyclopropenes and Nitriles via Azametallacyclopentadiene and η^2-Pyrimidine Metallacycle. J. Am. Chem. Soc. 2021, 143, 9151–9161. [PubMed: 34029479]
53. Gómez-Torres A; Aguilar-Calderón JR; Saucedo C; Jordan A; Metta-Magaña A; Pinter B; Fortier S Reversible oxidative-addition and reductive elimination of thiophene from a titanium complex and its thermally-induced hydrodesulphurization chemistry. Chem. Commun. 2020, 56, 1545–1548.
54. See XY; Beaumier EP; Davis-Gilbert ZW; Dunn PL; Pearce AJ; Wheeler TA; Tonks IA Generation of TiII Alkyne Trimerization Catalysts in the Absence of Strong Metal Reductants. Organometallics 2017, 36, 1383–1390. [PubMed: 28690352]

55. Ironically, we were initially using these complexes as synthons to make more complex Ti imidos. See:Adams N; Bigmore HR; Blundell TL; Boyd CL; Dubberley SR; Sealey AJ; Cowley AR; Skinner MEG; Mountford P New Titanium Imido Synthons: Syntheses and Supramolecular Structures. Inorg. Chem. 2005, 44, 2882–2894. [PubMed: 15819576]
56. DiFranco SA; Maciulis NA; Staples RJ; Batrice RJ; Odom AL Evaluation of Donor and Steric Properties of Anionic Ligands on High Valent Transition Metals. Inorg. Chem. 2012, 51, 1187–1200. [PubMed: 22200335]
57. Davis-Gilbert ZW; Kawakita K; Blechschmidt DC; Tsurugi H; Mashima K; Tonks IA In Situ Catalyst Generation and Benchtop-Compatible Entrypoints for Ti-Catalyzed Nitrene Transfer Reactions. Organometallics 2018, 37, 4439–4445. [PubMed: 31802785]
58. Pennington DA; Horton PN; Hursthouse MB; Bochmann M; Lancaster SJ Synthesis and catalytic activity of dinuclear imido titanium complexes: the molecular structure of [Ti(NPh)Cl(μ-Cl)(THF)2]2. Polyhedron 2005, 24, 151–156.
59. See XY; Wen X; Wheeler TA; Klein CK; Goodpaster JD; Reiner BR; Tonks IA Iterative Principal Component Analysis-Driven Ligand Design for Regioselective Ti-Catalyzed [2+2+1] Pyrrole Synthesis. ACS Catalysis 2020, 10, 13504–13517. [PubMed: 34327040]
60. Kawakita K; Beaumier EP; Kakiuichi Y; Tsurugi H; Tonks IA; Mashima K Bis(imido)vanadium(V)-Catalyzed [2+2+1] Coupling of Alkynes and Azobenzenes Giving Multi-Substituted Pyrroles. J. Am. Chem. Soc. 2019, 141, 4194–4198. [PubMed: 30731038]
61. Liang W; Nakajima K; Nishibayashi Y Synthesis of 1,2,4-azadiphosphole derivatives based on vanadium-catalyzed [2+2+1] cycloaddition reactions of azobenzenes with phosphaalkynes. RSC Adv. 2020, 10, 12730–12733.
62. Group 5 imido complexes often require a 2nd strong **π** donor to be activated toward cycloaddition. See: de With J; Horton AD Orpen AG Unusual [2 + 2] cycloaddition adducts of an imidovanadium complex with alkynes and ethene: conversion to .eta.3–1-azaallyl and ethenyl complexes. Organometallics 1993, 12, 1493–1496.
63. Cheng Y; Klein CK; Tonks IA Synthesis of Pentasubstituted 2-Aryl Pyrroles from Boryl and Stannyl Alkynes via One-Pot Sequential Ti-Catalyzed [2+2+1] Pyrrole Synthesis/Cross Coupling Reactions. Chem. Sci. 2020, 11, 10236–10242. [PubMed: 34094289]
64. Dallaire C; Brook MA The .beta.-effect with vinyl cations: kinetic study of the protiodemetalation of silyl-, germyl-, and stannylalkynes. Organometallics 1993, 12, 2332–2338.
65. Lefeber C; Ohff A; Tillack A; Baumann W; Kempe R; Burlakov VV; Rosenthal U Representation and regioselective reactions of the phosphine-free zirconocene-alkyne complex Cp2Zr(THF)(tBuC2 SiMe 3). J. Organomet. Chem. 1995, 501, 189–194.
66. List AK; Koo Kwangmo, Reingold AL; Hillhouse GL Preparation of trimethylsilyl alkyne complexes of bis(pentamethylcyclopentadienyl)zirconium, (η5-C5Me5)2Zr(RC≡CSiMe3), and their regioselective reactions with nitrous oxide. Inorg. Chim. Acta. 1998, 270, 399–404.
67. Micalizio GC; Mizoguchi H The Development of Alkoxide-Directed Metallacycle-Mediated Annulative Cross-Coupling Chemistry. Isr. J. Chem. 2017, 57, 228–238. [PubMed: 28652644]
68. Chiu H-C; See XY; Tonks IA Dative Directing Group Effects in Ti-Catalyzed [2+2+1] Pyrrole Synthesis: Chemo- and Regioselective Alkyne Heterocoupling. ACS Catal. 2019, 9, 216–223. [PubMed: 31768294]
69. Imbri D; Tauber J; Opatz T Synthetic Approaches to the Lamellarins—A Comprehensive Review. Mar. Drugs 2014, 12, 6142–6177. [PubMed: 25528958]
70. Hall A; Atkinson S; Brown SH; Chessell IP; Chowdhury A; Clayton NM; Coleman T; Giblin GMP; Gleave RJ; Hammond B; Healy MP; Johnson MR; Michel AD; Naylor A; Novelli R; Spalding DJ; Tang SP Structure−Activity Relationships of 1,5-Biaryl Pyrroles as EP1 Receptor Antagonists. Bioorg. Med. Chem. Lett. 2006, 16, 3657–3662. [PubMed: 16697196]
71. Gulevich AV; Dudnik AS; Chernyak N; Gevorgyan V Transition Metal-Mediated Synthesis of Monocyclic Aromatic Heterocycles. Chem. Rev. 2013, 113, 3084–3213. [PubMed: 23305185]
72. Davis-Gilbert ZW; Yao LJ; Tonks IA Ti-catalyzed Multicomponent Oxidative Carboamination of Alkynes with Alkenes and Diazenes. J. Am. Chem. Soc. 2016 138, 14570–14573. [PubMed: 27790910]

73. Guo J; Lu Y; Zhao R; Liu Z; Menberu W; Wang Z-X Strong Preference of the Redox-Neutral Mechanism over the Redox Mechanism for the Ti^{IV} Catalysis Involved in the Carboamination of Alkyne with Alkene and Diazene. Chem. Eur. J. 2018, 24, 7010–7025. [PubMed: 29709085]
74. Ruck RT; Zuckerman RL; Krska SW; Bergman RG Carboamination: Additions of Imine C=N Bonds Across Alkynes Catalyzed by Imidozirconium Complexes. Angew. Chem. Int. Ed. 2004, 43, 5372–5374.
75. Basuli F; Aneetha H; Huffman JC; Mindiola DJ A Fluorobenzene Adduct of Ti(IV), and Catalytic Carboamination to Prepare α,β-Unsaturated Imines and Triaryl-Substituted Quinolines. J. Am. Chem. Soc. 2005, 127, 17992–17993. [PubMed: 16366536]
76. Piou T; Rovis T Rhodium-catalysed *syn*-carboamination of alkenes via a transient directing group. Nature 2015, 527, 86–90. [PubMed: 26503048]
77. Liu Z; Wang Y; Wang Z; Zeng T; Liu P; Engle KM Catalytic Intermolecular Carboamination of Unactivated Alkenes via Directed Aminopalladation, J. Am. Chem. Soc. 2017, 139, 11261–11270. [PubMed: 28727452]
78. Gockel SN; Buchanan TL; Hull KL Cu-Catalyzed Three-Component Carboamination of Alkenes. J. Am. Chem. Soc. 2018, 140, 58–61. [PubMed: 29095598]
79. Neumann JJ; Suri M; Glorius F Efficient Synthesis of Pyrazoles: Oxidative C-C/N-N Bond-Formation Cascade. Angew. Chem., Int. Ed. 2010, 49, 7790–7794.
80. Diccianni JB; Hu C; Diao T N-N Bond Forming Reductive Elimination via a Mixed-Valent Nickel(II)-Nickel(III) Intermediate. Angew. Chem., Int. Ed. 2016, 55, 7534–7538.
81. Desnoyer AN; See XY; Tonks IA Diverse Reactivity of Diazatitanacyclohexenes: Coupling Reactions of 2H-Azirines Mediated by Titanium(II). Organometallics 2018, 37, 4327–4331. [PubMed: 31768086]
82. Frye CW; Egger DT; Kounalis E; Pearce AJ; Cheng Y; Tonks IA α-Diimine Synthesis via Titanium-Mediated Multicomponent Diimination of Alkynes with C-Nitrosos. ChemRxiv 2021, DOI: 10.33774/chemrxiv-2021-dmdqr.
83. Smolensky E; Kapon M; Eisen MS Catalytic Intermolecular Hydroamination of Methylenecyclopropanes. Organometallics 2005, 24, 5495–5498.
84. Smolensky E; Kapon M; Eisen MS Intermolecular Hydroamination of Methylenecyclopropane Catalyzed by Group IV Metal Complexes. Organometallics 2007, 26, 4510–4527.
85. Beaumier EP; Ott AA; Wen X; Davis-Gilbert ZW; Wheeler TA; Topczewski JJ; Goodpaster JD; Tonks IA Ring-Opening Oxidative Amination of Methylenecyclopropanes with Diazenes via Ti^{II}/Ti^{IV} Redox Catalysis. Chem. Sci. 2020, 11, 7204–7209. [PubMed: 34123005]
86. Munhá RF; Zarkesh RA; Heyduk AF Group transfer reactions of d0 transition metal complexes: redox-active ligands provide a mechanism for expanded reactivity. Dalton Trans. 2013, 42, 3751–3766. [PubMed: 23334157]
87. Nguyen AI; Zarkesh RA; Lacy DC; Thorson MK; Heyduk AF Catalytic nitrene transfer by a zirconium(iv) redox-active ligand complex. Chem. Sci. 2011, 2, 166–169.
88. Heins SP; Wolczanski PT; Cundari TR; MacMillan SN Redox non-innocence permits catalytic nitrene carbonylation by (dadi)Ti=NAd (Ad = adamantyl). Chem. Sci. 2017, 8, 3410–3418. [PubMed: 28507712]
89. Beaumier EP; McGreal M; Pancoast AR; Wilson RH; Moore JT; Graziano BJ; Goodpaster JD; Tonks IA Carbodiimide Synthesis via Ti-Catalyzed Nitrene Transfer from Diazenes to Isocyanides. ACS Catal. 2019, 9, 11753–11762. [PubMed: 34113477]

KEY REFERENCES

- Gilbert, Z. W.; Hue, R. J.; Tonks, I. A. Catalytic Formal [2+2+1] Synthesis of Pyrroles from Alkynes and Diazenes via Ti^{II}/Ti^{IV} Redox Catalysis. *Nature Chemistry* **2016**, *8*, 63–68. *We report the first example catalytic oxidative nitrene transfer with Ti, leading to the formation of pyrroles.*[1]
- Davis-Gilbert, Z. W.; Wen, X.; Goodpaster, J. D.; Tonks, I. A. Mechanism of Ti-Catalyzed Oxidative Nitrene Transfer in [2+2+1] Pyrrole Synthesis. *J. Am. Chem. Soc.* **2018**, *140*, 7267–7281. *A detailed combined experimental and theoretical study of the mechanism of Ti-catalyzed oxidative amination, revealing a new electrocyclic mechanism for C-N reductive elimination and kinetic and mechanistic details regarding the overall catalytic cycle.*[2]
- Chiu, H.-C.; Tonks, I. A. Trialkylsilyl-Protected Alkynes as Selective Cross Coupling Partners in Ti-Catalyzed [2+2+1] Pyrrole Synthesis. *Angew. Chem. Int. Ed.* **2018**, *57*, 6090–6094. *The first example of selective multicomponent reactions of Ti imidos and alkynes with 3rd components, in this case yielding highly regioselective reactions for the formation of silyl pyrroles. These pyrroles were then used as precursors to the natural product Lamellarin R.*[3]
- Pearce, A. J.; Harkins, R. P.; Reiner, B. R.; Wotal, A. C.; Dunscomb, R. J.; Tonks, I. A. Multicomponent Pyrazole Synthesis from Alkynes, Nitriles, and Titanium Imido Complexes *via* Oxidatively-Induced N-N Bond Coupling. *J. Am. Chem. Soc.* **2020**, *142*, 4390. *Demonstration of a useful multicomponent pyrazole synthesis through N-N coupling chemistry, taking advantage of our understanding of selective insertion into azatitanacycles and electrocyclic reductive elimination reactions.*[4]

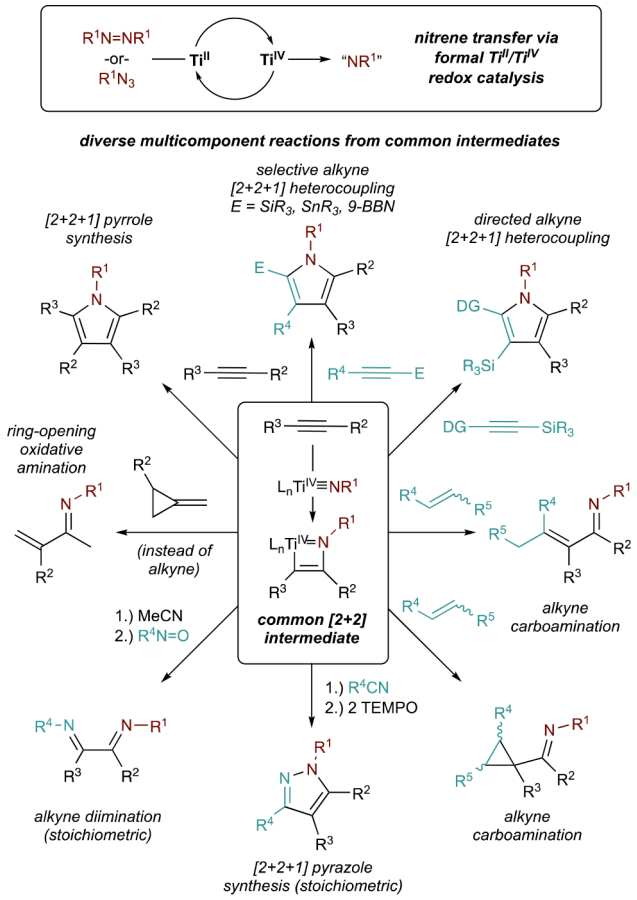

Figure 1.

Summary of oxidative amination reactions catalyzed or mediated by Ti imido (Ti≡NR) complexes.

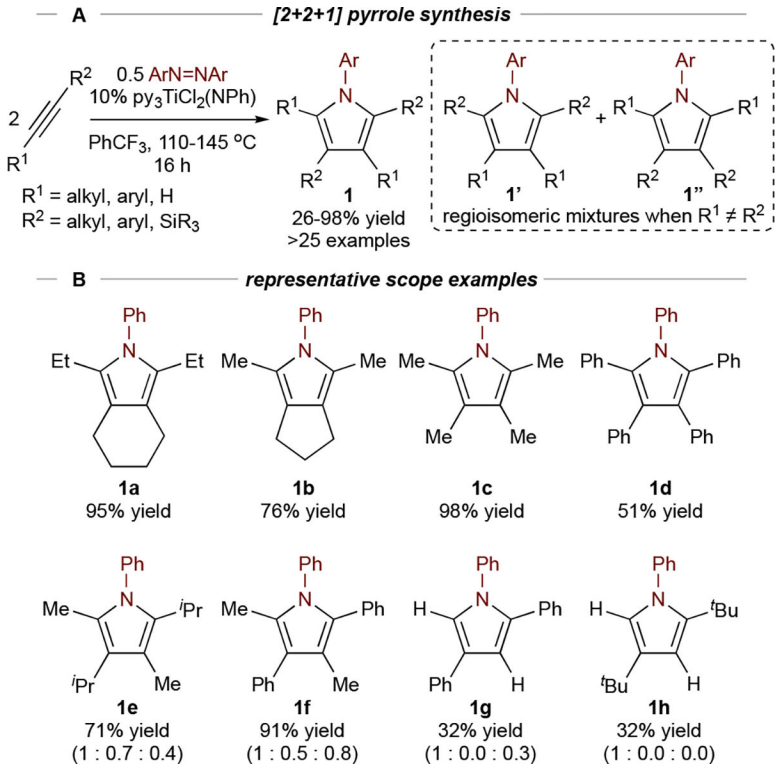

Figure 2.

Initial demonstration of Ti^{II}/Ti^{IV}-catalyzed synthesis of pyrroles along with representative examples. Regioisomeric ratios (**1** : **1'** : **1"**) in parentheses.

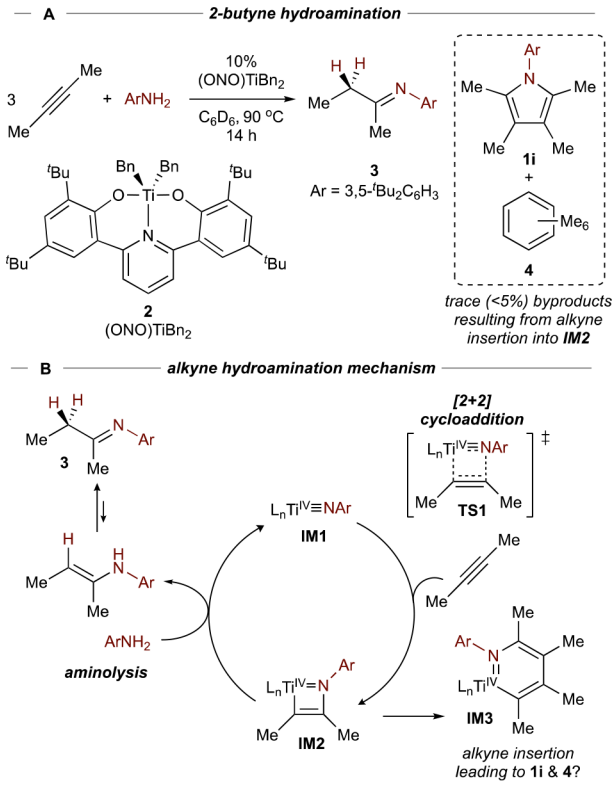

Figure 3.

Earlier studies of 2-butyne hydroamination led to the observation of minor byproducts resulting from 2nd alkyne insertion into **IM2**.

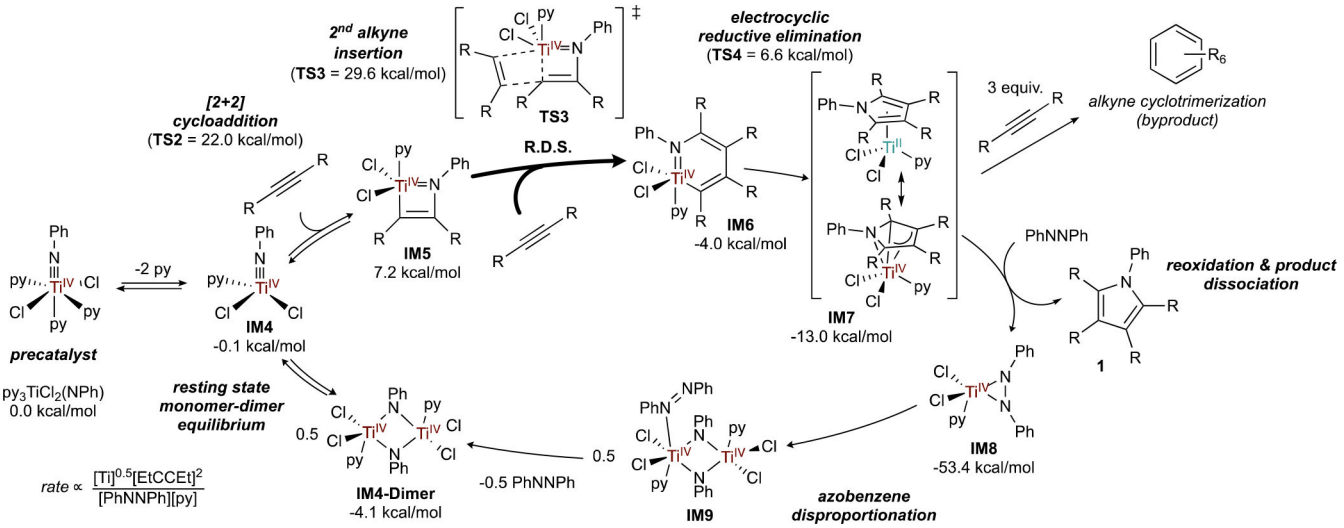

Figure 4.

Mechanism of $py_3TiCl_2(NPh)$-catalyzed [2+2+1] pyrrole synthesis. Computed free energies (M06/6–311G(d,p)/SMD, $PhCF_3$, 115 °C) for R = Me. Reaction energy span reads from **IM4-Dimer** to **IM8**.

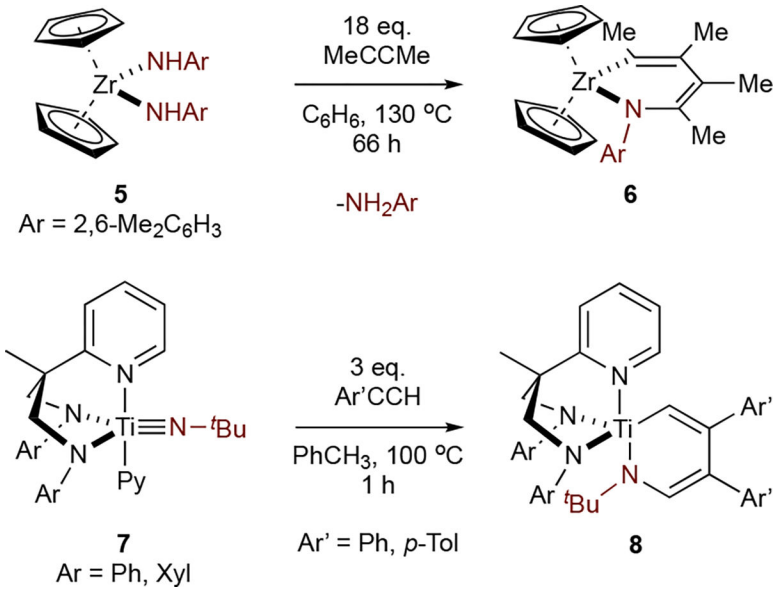

Figure 5.
Examples of group 4 imidos that undergo reaction with 2 equivalents of alkyne.

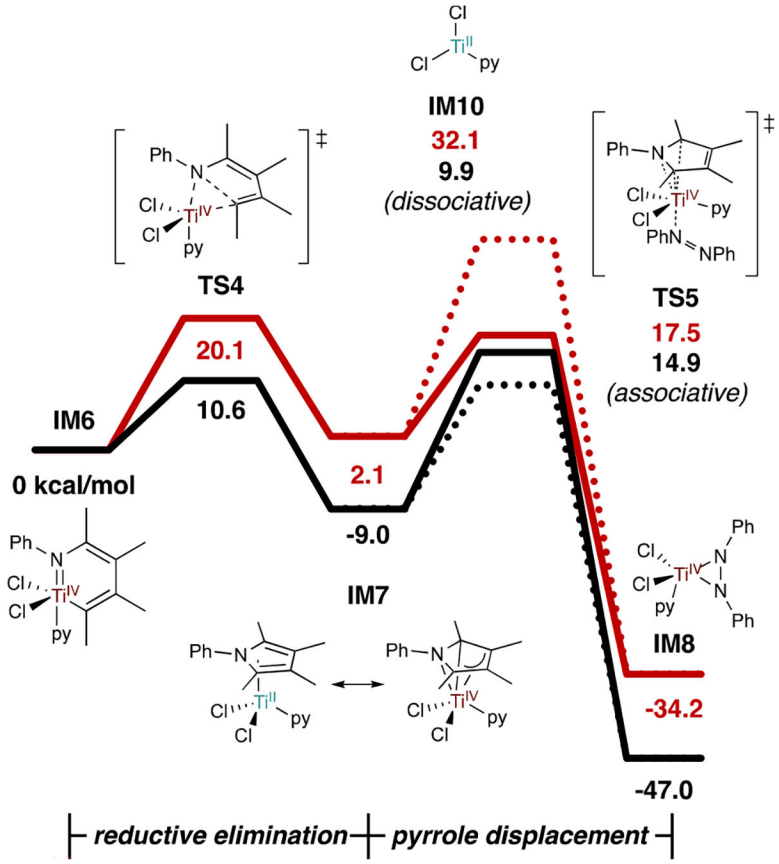

Figure 6.

Computational free energies of reductive elimination and pyrrole displacement/reoxidation by PhNNPh. Black lines (M06/6–311G(d,p)/SMD, $PhCF_3$, 115 °C) from ref 20. Red lines (gas-phase B3LYP/6–311G(d,p) followed by SPE at M06-L/6–311++G(d,p)/PCM, $PhCF_3$, 25 °C) from ref 22. Solid lines follow associative exchange of pyrrole by PhNNPh (**TS5**); dotted lines follow dissociative exchange (**IM10**).

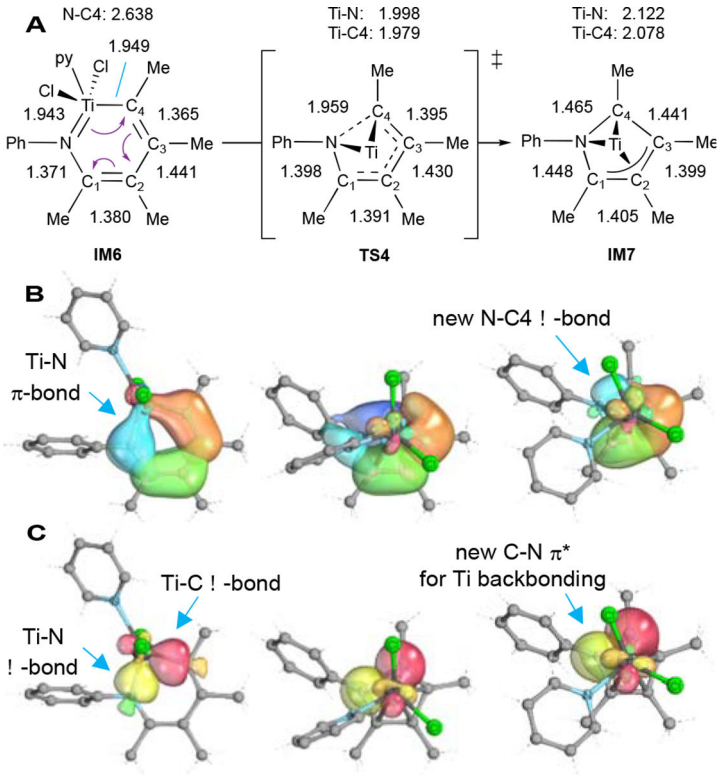

Figure 7.

(A) Calculated bond lengths (Å) and IBOs (B and C) for reductive elimination from **IM6** (left) through **TS4** (middle) to **IM7** (right). Figure adapted from ref 2.

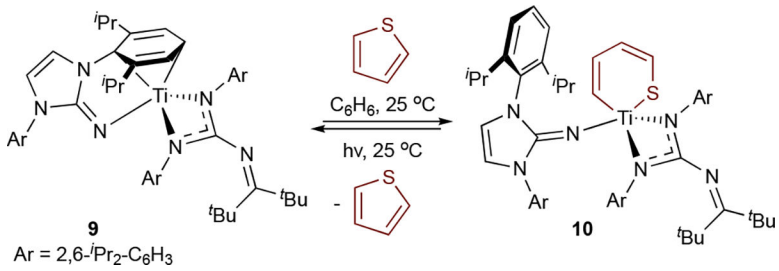

Figure 8.
Reversible oxidative addition/reductive elimination of thiophene to a masked Ti^{II} complex.

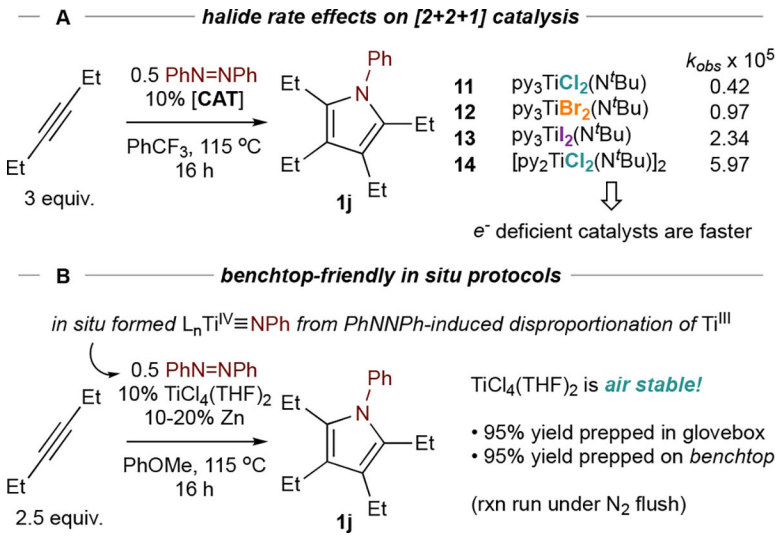

Figure 9.

Halide and pyridine effects on the rate of [2+2+1] pyrrole formation. Bottom: *in situ* catalysts from air-stable $TiCl_4(THF)_2$ provide a convenient entrypoint into catalysis.

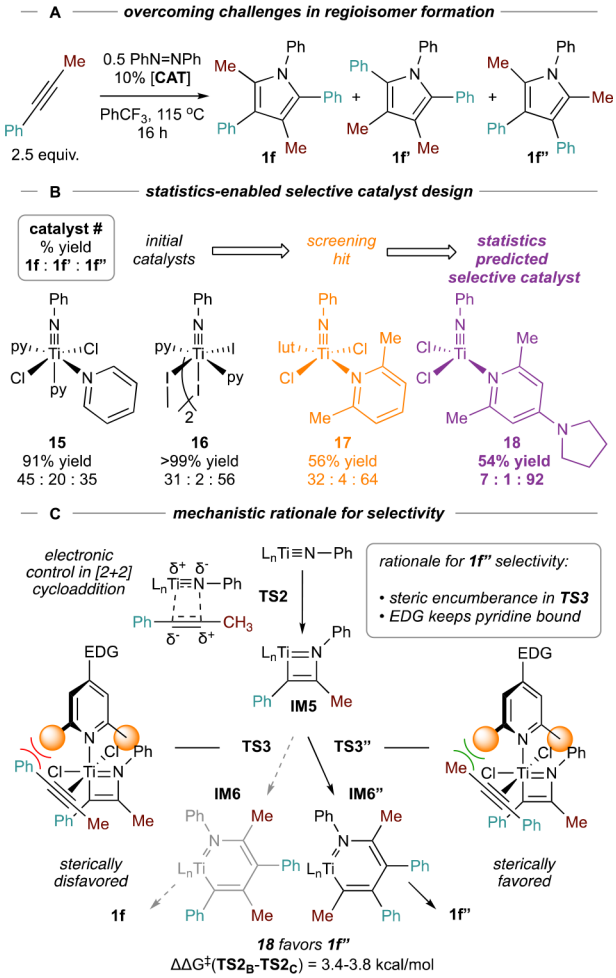

Figure 10.
Design of regioselective catalysts for [2+2+1] pyrrole synthesis from phenylpropyne.

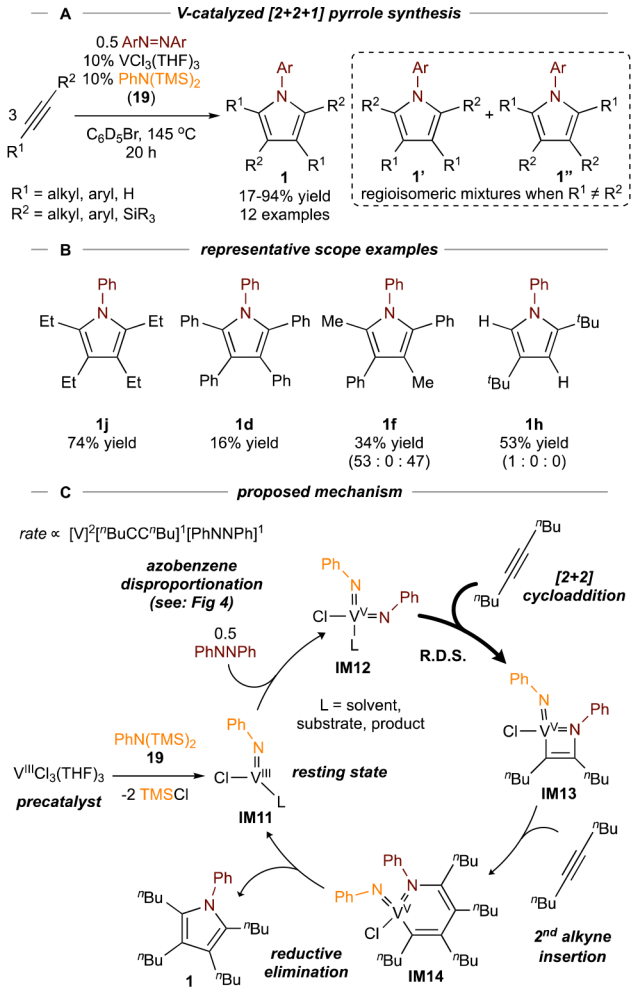

Figure 11.
V-catalyzed [2+2+1] pyrrole synthesis from alkynes and azobenzene.

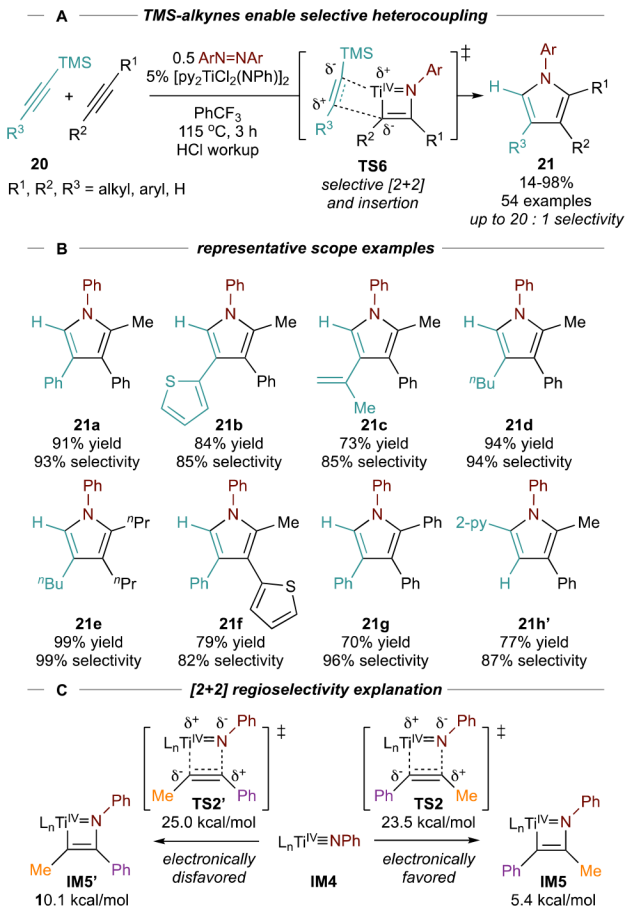

Figure 12.

Chemoselective [2+2+1] alkyne heterocouplings with TMS-substituted alkynes. L_n = $pyCl_2$.

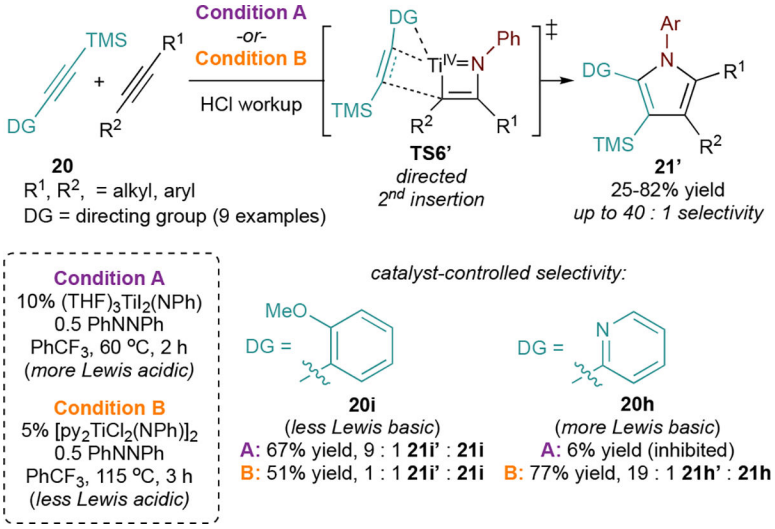

Figure 13.

Directing group effects can invert regioselectivity in [2+2+1] alkyne heterocoupling reactions. Structure of **21** shown in Figure 12.

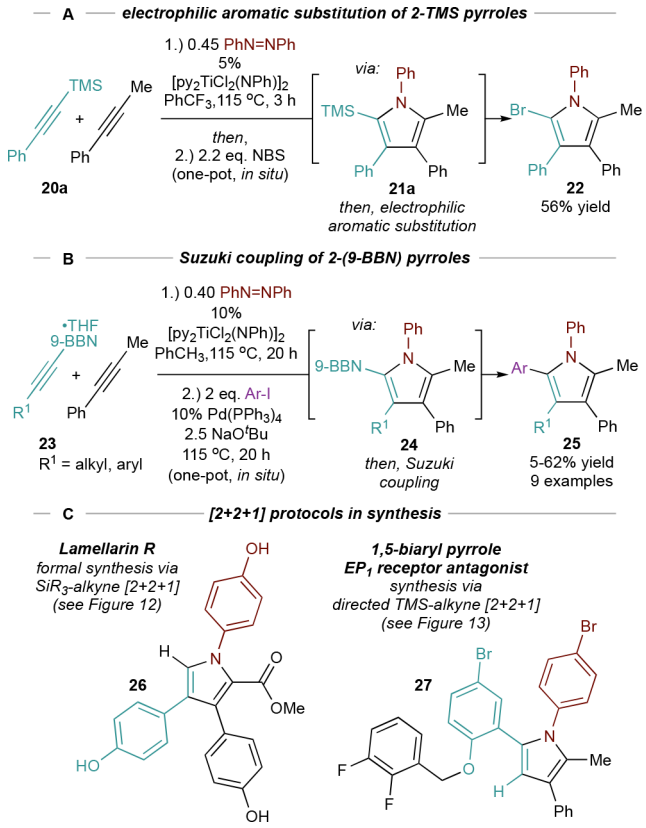

Figure 14.

Heteroatom-substituted pyrroles provide convenient handles for further functionalization and can be used in synthesis.

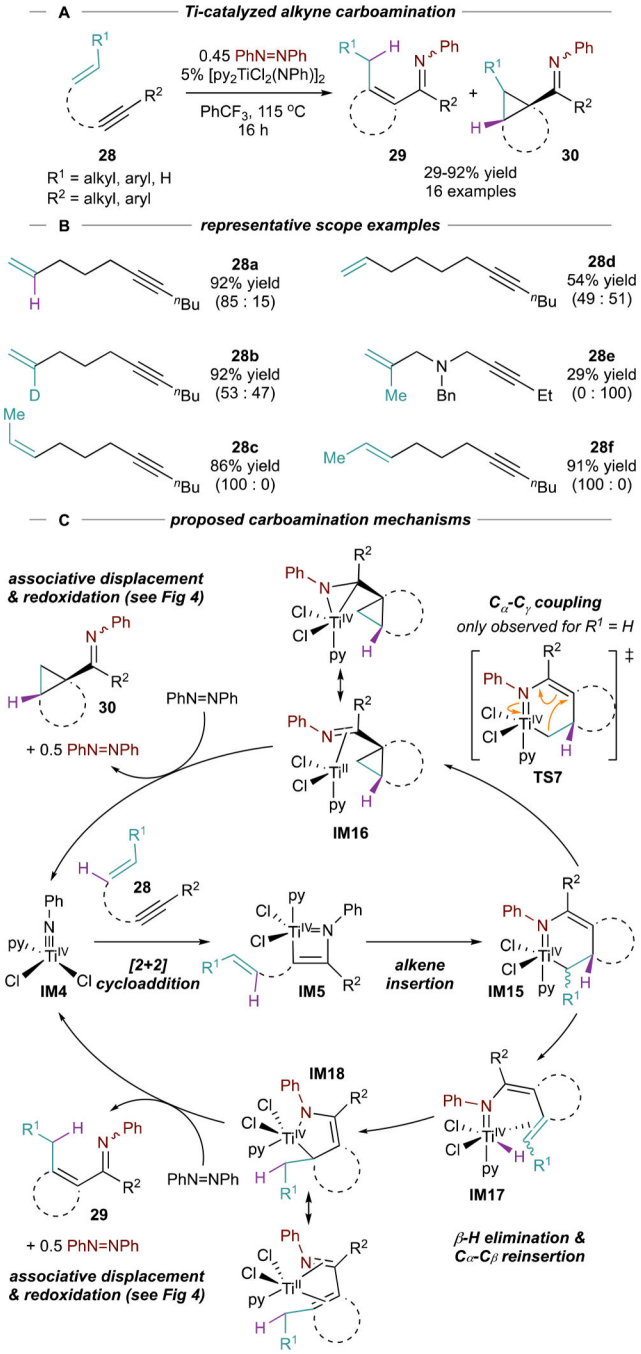

Figure 15.

Ti-catalyzed oxidative carboamination of alkynes with alkenes and azobenzene, along with mechanism showing divergent pathways to **29** and **30**. Regioisomeric ratios (**29**:**30**) reported in parentheses. Purple β-H in **28** tracked throughout for clarity.

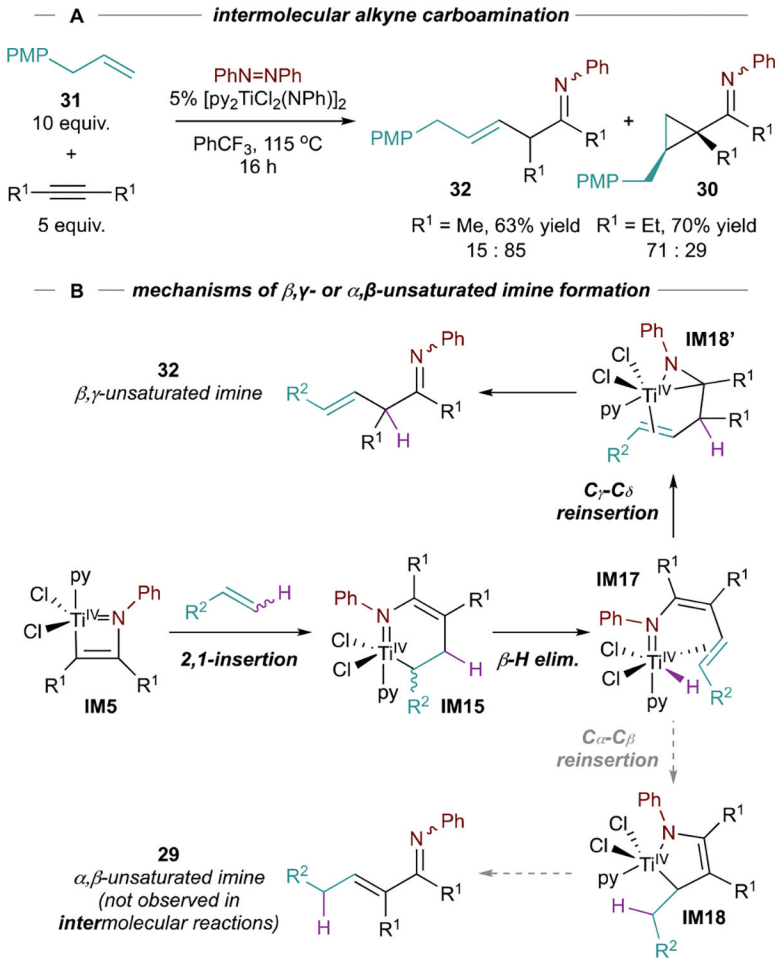

Figure 16.

Intermolecular carboamination leads to β,γ-unsaturated imine **32** instead of α,β-unsaturated **29** resulting from differential Ti-H reinsertion in **IM17**. PMP = *para*-methoxyl-phenyl.

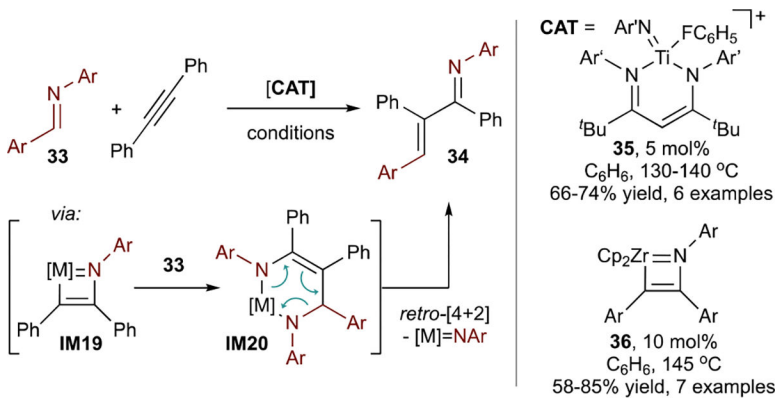

Figure 17.

Examples of group 4 imido-catalyzed alkyne carboamination *via* a redox-neutral mechanism.

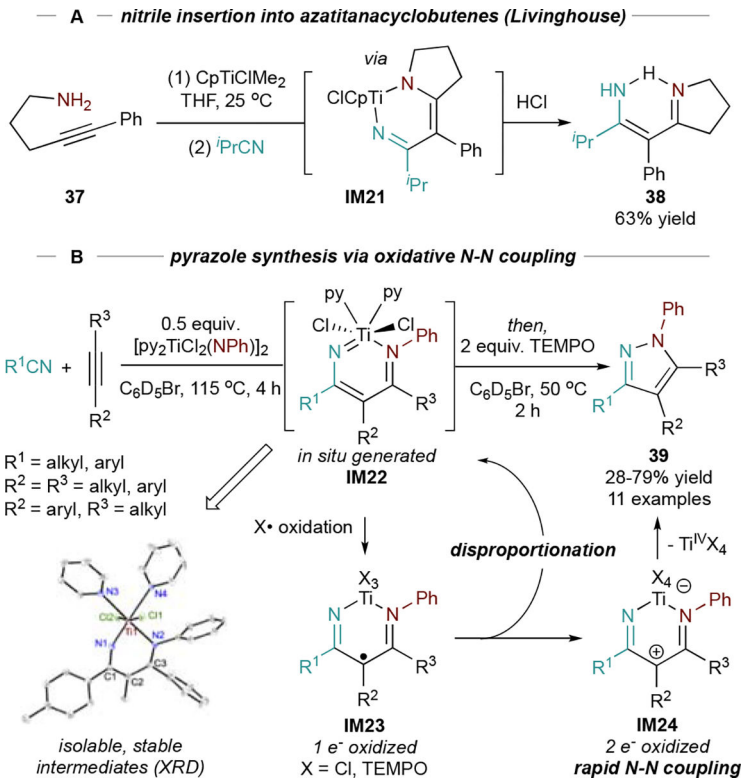

Figure 18.

A: precedent for stoichiometric isobutyronitrile insertion into [2+2] cycloadducts. B: multicomponent pyrazole synthesis *via* oxidation-induced N-N coupling.

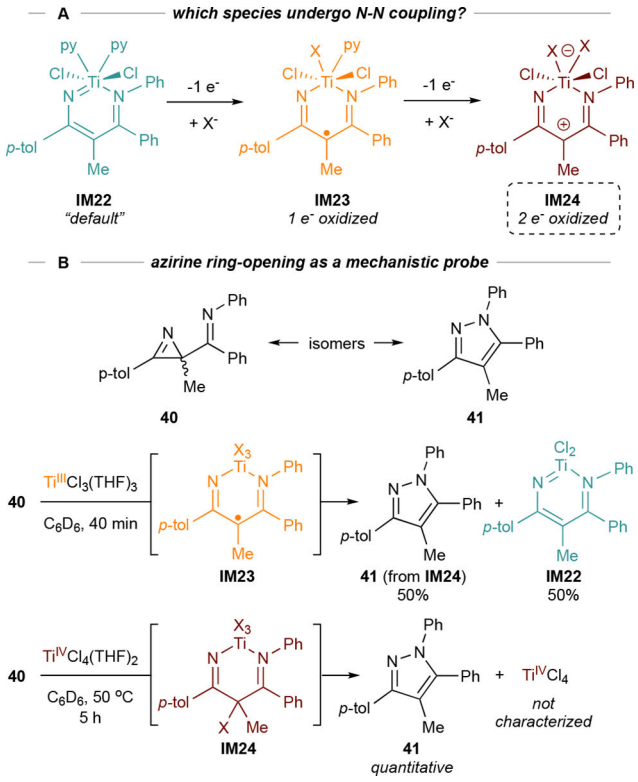

Figure 19.

2*H*-azirine ring-opening with various oxidation states of Ti reveals that N-N coupling occurs through a 2e-oxidized species **IM24**, although 1-electron oxidized **IM23** can also disproportionate into **IM24**.

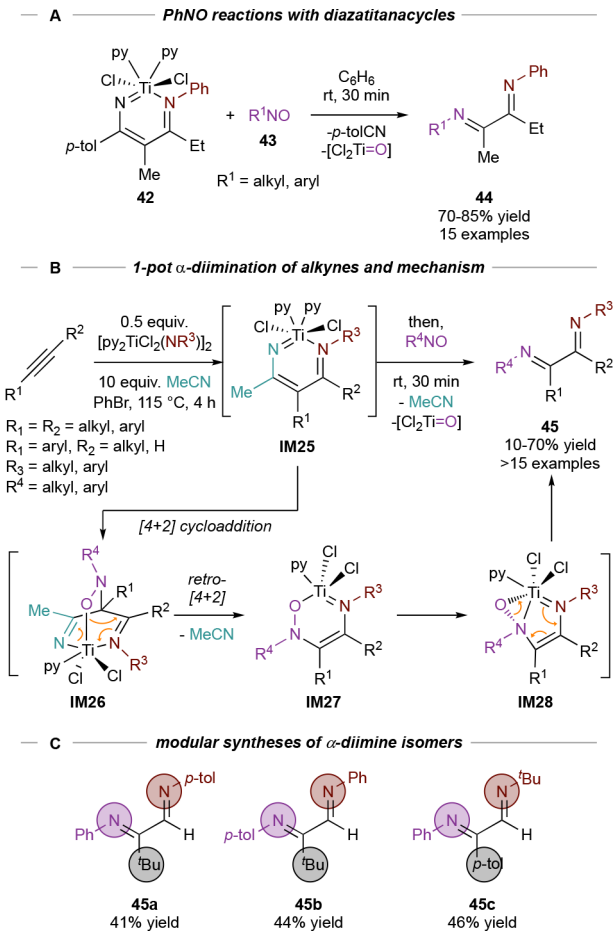

Figure 20.
Development of stoichiometric Ti- and nitrile-mediated alkyne α-diimination.

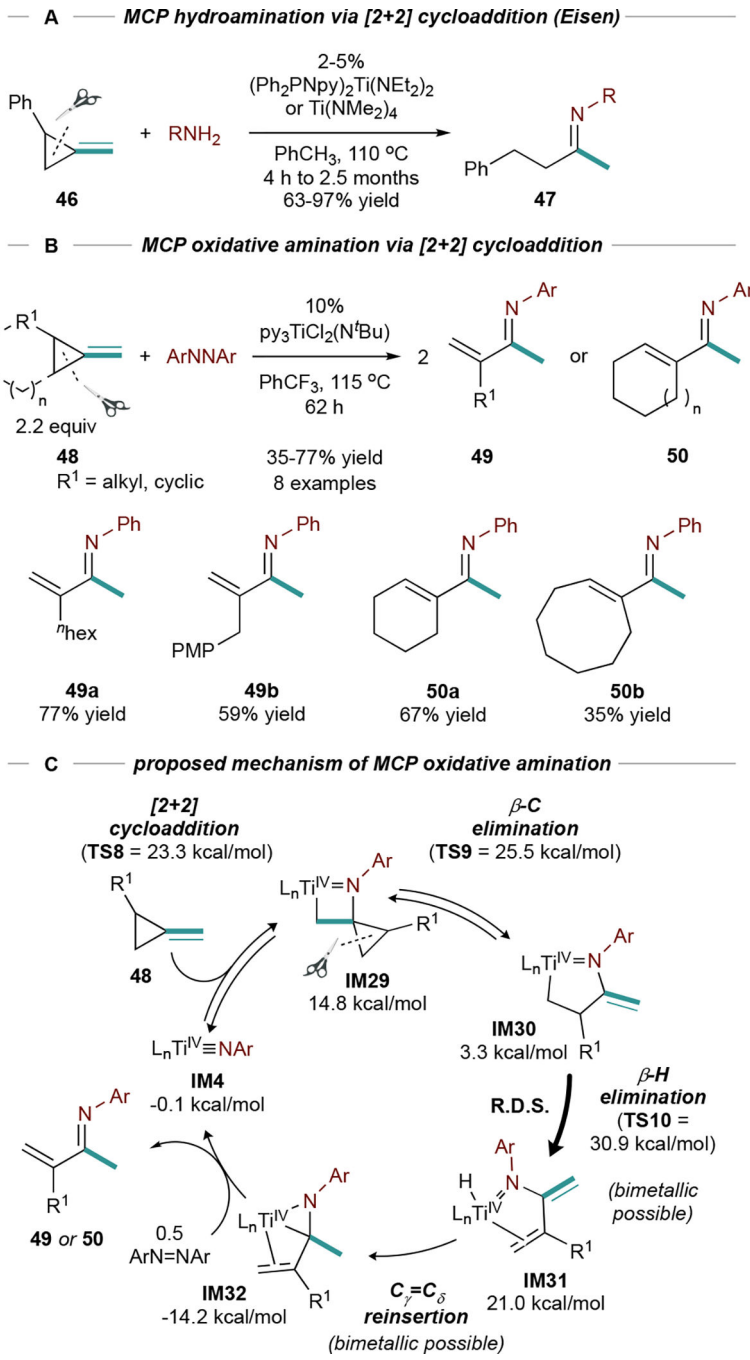

Figure 21.

Hydroamination and oxidative amination of methylene cyclopropanes (MCPs). Isolated yields. PMP = *para*-methoxyl-phenyl.

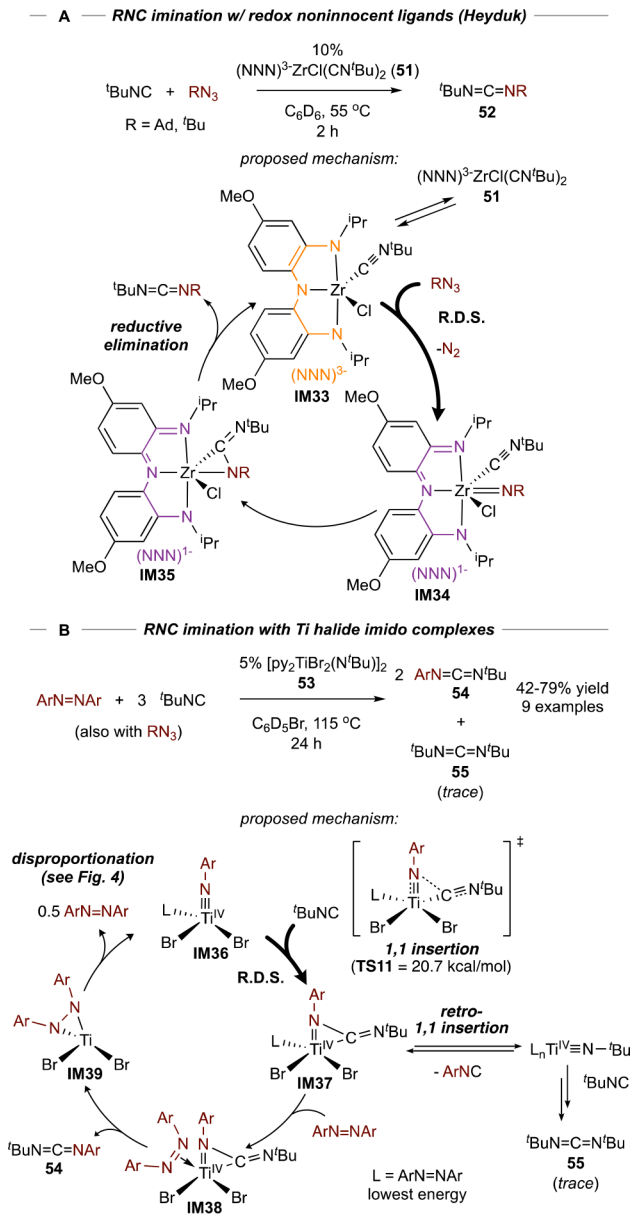

Figure 22.

Examples of catalytic carbodiimide formation via isocyanide imination redox noninnocent Zr complexes (A) and Ti halide complexes (B).